Received: 4 December 2020 | Revised: 4 June 2021 | Accepted: 5 June 2021

DOI: 10.1111/mmi.14768

RESEARCH ARTICLE

WILEY

Minor pilins are involved in motility and natural competence in the cyanobacterium *Synechocystis* sp. PCC 6803

Sabrina Oeser[1] | Thomas Wallner[1] | Nils Schuergers[1] | Lenka Bučinská[2] | Shamphavi Sivabalasarma[3,4] | Heike Bähre[5] | Sonja-Verena Albers[3,4] | Annegret Wilde[1]

[1]Molecular Genetics, Institute of Biology III, University of Freiburg, Freiburg, Germany

[2]Centre Algatech, Institute of Microbiology of the Czech Academy of Sciences, Trebon, Czech Republic

[3]Molecular Biology of Archaea, Institute of Biology II, University of Freiburg, Freiburg, Germany

[4]Spemann Graduate School of Biology and Medicine, University of Freiburg, Freiburg, Germany

[5]Research Core Unit Metabolomics, Medical School Hannover, Hannover, Germany

Correspondence
Annegret Wilde, Molecular Genetics, Institute of Biology III, University of Freiburg, Freiburg, Germany.
Email: annegret.wilde@biologie.uni-freiburg.de

Funding information
This work was supported by grants to AW and SVA in frame of the SFB 1381 by the Deutsche Forschungsgemeinschaft (German Research Foundation) under project no. 403222702-SFB 1381 (A1, A2) and to AW as part of DFG Priority Programme SPP1879 (Wi 2014/7-1)

Abstract

Cyanobacteria synthesize type IV pili, which are known to be essential for motility, adhesion and natural competence. They consist of long flexible fibers that are primarily composed of the major pilin PilA1 in *Synechocystis* sp. PCC 6803. In addition, *Synechocystis* encodes less abundant pilin-like proteins, which are known as minor pilins. In this study, we show that the minor pilin PilA5 is essential for natural transformation but is dispensable for motility and flocculation. In contrast, a set of minor pilins encoded by the *pilA9-slr2019* transcriptional unit are necessary for motility but are dispensable for natural transformation. Neither *pilA5-pilA6* nor *pilA9-slr2019* are essential for pilus assembly as mutant strains showed type IV pili on the cell surface. Three further gene products with similarity to PilX-like minor pilins have a function in flocculation of *Synechocystis*. The results of our study indicate that different minor pilins facilitate distinct pilus functions. Further, our microarray analysis demonstrated that the transcription levels of the minor pilin genes change in response to surface contact. A total of 122 genes were determined to have altered transcription between planktonic and surface growth, including several plasmid genes which are involved exopolysaccharide synthesis and the formation of bloom-like aggregates.

KEYWORDS
cyanobacteria, minor pilin, natural competence, surface acclimation, type IV pili

1 | INTRODUCTION

The unicellular, coccoidal cyanobacterium *Synechocystis* sp. PCC 6803 (hereinafter designated *Synechocystis*) carries two types of cell appendages—thin pili with diameters of 2–3 nm and lengths of 0.5–1 μm and thick pili with diameters of 6–8 nm and possible lengths well beyond 1 μm (Bhaya et al., 2000). Whereas the composition and role of thin pili has not been elucidated, genetic and phylogenetic analyses have demonstrated that the thick pili are type IV pili (T4P) (Bhaya et al., 1999, 2000; Yoshihara et al., 2001), which are classified as type IVa pili (T4aP) (Denise et al., 2019). In *Synechocystis*, T4aP are involved in cell adhesion (Nakane & Nishizaka, 2017), cell-cell aggregation (Conradi et al., 2019), natural transformation (Yoshihara et al., 2001), and twitching motility—a jerky motion on surfaces (Bhaya et al., 2000; Mattick, 2002).

The core components of T4P are widely conserved across different prokaryotic phyla (Denise et al., 2019). T4aP subunits of *Synechocystis* have been identified by homology to *Pseudomonas*

aeruginosa (hereinafter designated *Pseudomonas*) and *Myxococcus xanthus* (hereinafter designated *Myxococcus*) pilus proteins (Bhaya et al., 1999, 2000; Yoshihara et al., 2001). PilQ is an integral outer membrane secretin and enables the emergence of the extending pilus fiber. The pilus platform is formed by the integral inner membrane protein PilC and traffic ATPases that facilitate the extension (PilB) or retraction (PilT) of the fiber. The PilMNO proteins align the pilus components throughout the periplasm. The most abundant structural protein of the pilus fiber is the major pilin PilA. PilA prepilins are inserted into the inner membrane, where they are processed by the bifunctional leader peptidase/methylase PilD and are subsequently inserted into the growing fiber (reviewed in Pelicic, 2008). In addition to the highly abundant major pilin, T4P-forming bacteria usually encode several, less abundant minor pilins with different functions. Minor pilin genes are often clustered and specific subsets of genes are differentially expressed and likely coregulated. The *Myxococcus* genome contains three gene clusters each encoding a variant of the adhesin PilY1 and four minor pilins, the so-called core minor pilins. These form a priming complex which is essential for T4aP pilus assembly. The complex of the minor pilins and PilY1 locates at the tip of the extended pilus and promotes adhesion to a surface (Treuner-Lange et al., 2020). In *Pseudomonas*, a similar minor pilin operon consisting of seven genes is under control of the transcription factor AlgR (Belete et al., 2008). The encoded set of minor pilins together with PilY1 was also suggested to function in pilus assembly (Nguyen et al., 2015) and to be incorporated into the pilus filament (Giltner et al., 2010). Further specific minor pilins (also called non-core minor pilins, Jacobsen et al., 2020) are involved in diverse pilus functions, such as aggregation, adhesion and natural transformation, in various bacteria (Ng et al., 2016; Winther-Larsen et al., 2001; Wolfgang et al., 1999), including the cyanobacterium *Synechococcus elongatus* PCC 7942 (Taton et al., 2020). The involvement of specialized minor pilins in DNA binding at the T4P tip was demonstrated for *Vibrio cholerae* (Ellison et al., 2018). In addition, the pilin-like proteins ComP of *Neisseria meningitidis* (Cehovin et al., 2013) and ComZ of *Thermus thermophilus* (Salleh et al., 2019) were suggested to interact with DNA at the pilus tip. Notably, these pilins are important for natural transformation but not for piliation.

Synechocystis encodes at least nine minor pilins, PilA2-PilA11. PilA3 was misidentified and is now considered a Tat protein that has characteristics of both TatA and TatB of the Tat protein secretion system (Aldridge et al., 2008). All major and minor pilins contain a conserved PilD cleavage site (G|XXXXE) followed by a hydrophobic stretch (Linhartová et al., 2014). Most minor pilin genes of *Synechocystis* are organized in operons (Figure 1a). Based on the transcriptomic data by Kopf et al. (2014), the transcriptional unit (TU) *TU763* comprises a polycistronic mRNA encoding the minor pilins PilA9, PilA10 and PilA11 together with the open reading frames *slr2018* and *slr2019*. The minor pilin genes *pilA5* and *pilA6* constitute *TU2300*. The downstream *pilA7* and *pilA8* genes are most likely transcribed from a different promoter. To date, knowledge regarding minor pilin function in *Synechocystis* is scarce. Deletion mutants of *pilA1*, *pilA10* and *pilA11* are non-motile on agar plates (Bhaya et al., 2001; Yoshihara et al., 2001). Furthermore, it was demonstrated that deletion of the whole *pilA9-slr2019* genomic region not only leads to loss of motility (Wallner et al., 2020) but also impairs flocculation (Conradi et al., 2019), which describes the aggregation of cells into floating assemblages in liquid culture. Hu et al. (2018) showed, that the antisense RNA PilR negatively regulates the amount of *pilA11* mRNA and the corresponding protein. Thus, overexpression of the antisense RNA led to inhibition of motility in this study. In another study it was shown that PilA4 co-localizes with the pilus fiber if the major pilin PilA1 is present (Cengic et al., 2018).

As in many other bacteria, a functional T4P system is crucial for natural competence of *Synechocystis* (Yoshihara et al., 2001). The uptake mechanism has not been fully elucidated, but it is known that DNA is processed to a single-stranded form during DNA uptake (Barten & Lill, 1995) and that homologs of the proteins ComA (Slr0197) (Yoshihara et al., 2001; Yura et al., 1999) and ComF (Slr0388) (Nakasugi et al., 2006) are important for competence of *Synechocystis* cells. A protein with homology to ComEC was identified by Yoshihara et al. (2001), but they were not able to inactivate the corresponding gene *sll1929*.

T4P are also involved in surface attachment and biofilm formation, which are important in the life of many prokaryotes. Biofilms confer a fitness advantage over planktonic solitary cells by protection from diverse environmental stresses, better nutrient availability and drug and predator resistance (Laventie & Jenal, 2020). Surface recognition by different appendages, including T4P, triggers signal transduction cascades involving second messengers, quorum-sensing systems, two-component systems and small regulatory RNAs (Laventie & Jenal, 2020). For *Pseudomonas*, which possesses T4aP and a single polar flagellum, it was suggested that pilus tension leads to conformational change of the T4P, which subsequently leads to 3′,5′-cyclic adenosine monophosphate (cAMP) production and activation of virulence programmes (Persat et al., 2015). Additionally, surface contact of the flagellum (Laventie et al., 2019), as well as surface adhesion of PilY1 together with a functional T4P (Rodesney et al., 2017), trigger the production of 3′,5′-cyclic dimeric guanosine monophosphate (c-di-GMP). Increased c-di-GMP levels promote surface acclimation by inhibiting flagella motility, thereby promoting faster T4P-dependent surface attachment and production of extracellular polymeric substances (EPS) (Rodesney et al., 2017).

For *Synechocystis*, little is known regarding surface sensing and the transition from planktonic to sessile lifestyle. However, *Synechocystis* encodes cAMP- and c-di-GMP-dependent signalling components (Agostoni et al., 2013; Ohmori & Okamoto, 2004). Intracellular c-di-GMP levels can alter cellular deposition (Agostoni et al., 2016) and control flocculation (Conradi et al., 2019) and motility (Savakis et al., 2012). Motility is also dependent on cAMP, as inactivation of the adenylate cyclase gene *cya1* leads to inhibition of phototaxis on agar plates (Terauchi & Ohmori, 1999).

In this study, we investigate the role of minor pilins in *Synechocystis* and show that the minor pilin PilA5 is involved in natural competence. Furthermore, our data imply that among others, genes encoding minor pilins, cell envelope structures and genes located on

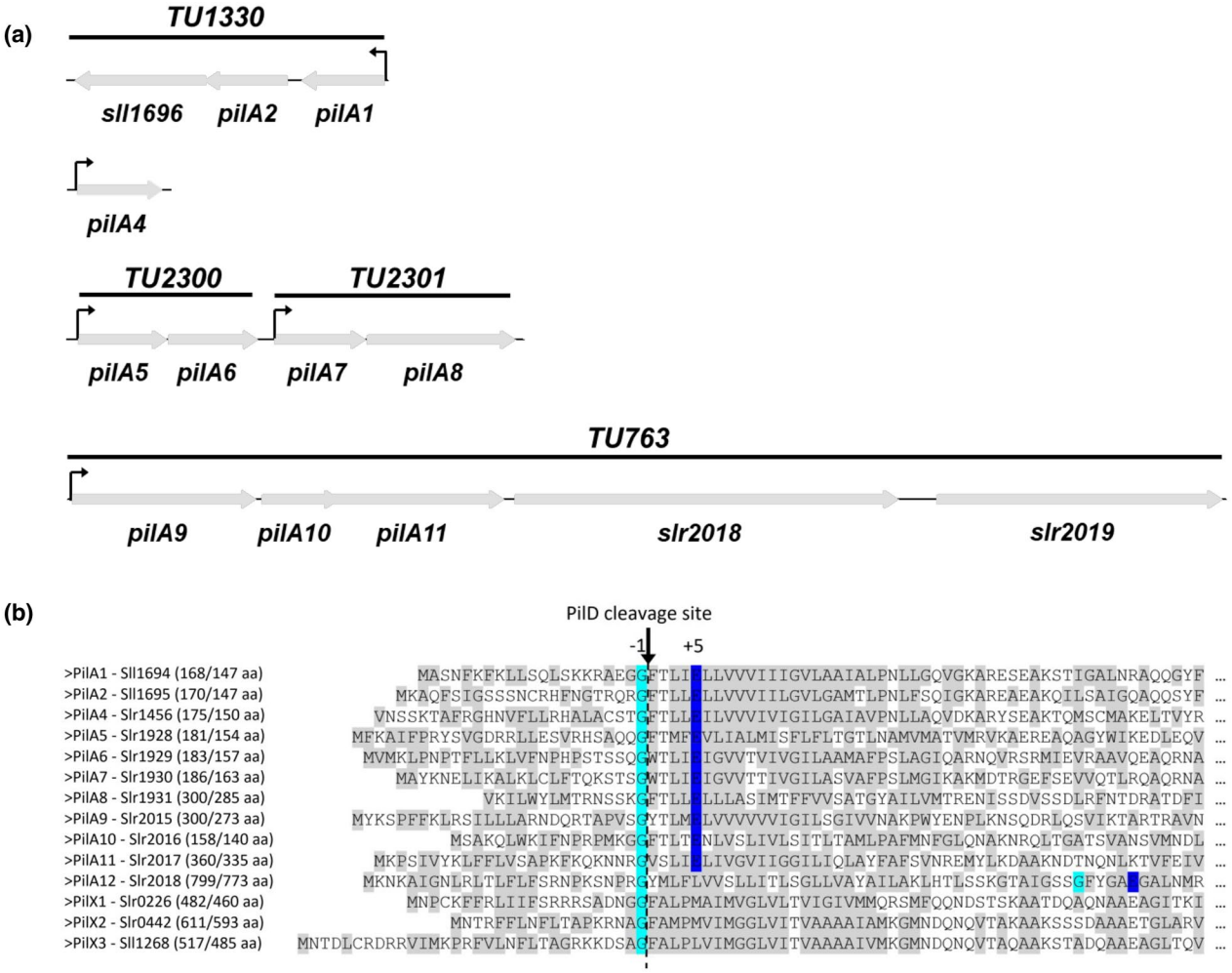

FIGURE 1 Major and minor pilins of *Synechocystis*. (a) Schematic representation of *Synechocystis* gene clusters encoding PilA1 and minor pilins. PilX homologues *slr0226*, *slr0442* and *sll1268* are not encoded in an operon or in proximity to other pilins. The proteins encoded by *sll1696* of *TU1330* and *slr2019* of *TU763* are not minor pilins. (b) Multiple alignment of the major pilin PilA1 and the proposed minor pilins. The potential cleavage site by PilD is marked with the dotted line and an arrow. The conserved glycine and glutamate at positions −1 and +5 in relation to the cleavage site are highlighted in turquois and blue, respectively. The newly proposed minor pilins PilA12 (Slr2018), Slr0226, Slr0442, and Sll1268 contain a hydrophobic amino acid substitution at position +5. The length of the full-length protein/mature protein is given next to the protein name in brackets. Hydrophobic amino acid residues are highlighted in grey

the plasmid pSYSM are major targets of a putative surface sensing system. We also investigated changes in second messenger production upon surface contact.

2 | RESULTS

2.1 | Minor pilins play roles in motility and surface attachment

In addition to the major pilin PilA1, *Synechocystis* encodes at least nine different minor pilins (Linhartová et al., 2014). Considering that the *TU2300*, encoding the minor pilins PilA5, PilA6 and the *TU763*, encoding PilA9, PilA10, PilA11 together with the hypothetical proteins Slr2018 and Slr2019, are inversely regulated in response to blue light (Wallner et al., 2020), we questioned if these sets of minor pilins are involved in different pilus functions. In contrast to the Δ*pilA9-slr2019* mutant, which is non-motile, a Δ*pilA5-pilA6* mutant strain showed a clear phototaxis response (Wallner et al., 2020). To identify other phenotypes, we first tested whether the Δ*pilA5-pilA6* strain is impaired in flocculation. Figure 2 shows that the Δ*pilA5-pilA6* strain exhibits a WT flocculation response and clearly differs from the non-flocculating and non-motile Δ*pilA9-slr2019* and Δ*hfq* mutant strains (Conradi et al., 2019; Wallner et al., 2020). The Δ*hfq* strain was employed as a control. The function of the cyanobacterial homologue of the RNA chaperone Hfq is not well understood yet. However, it is known that deletion or mutation of the *hfq* gene in *Synechocystis* led to transcriptional changes of many genes, including minor pilin genes, several ncRNAs and the CRISPR systems and therefore this mutant seems to be dysregulated in many ways (Dienst et al., 2008). Hfq is an interaction partner of the secretion ATPase PilB1 and seems to co-localize with the pilus base

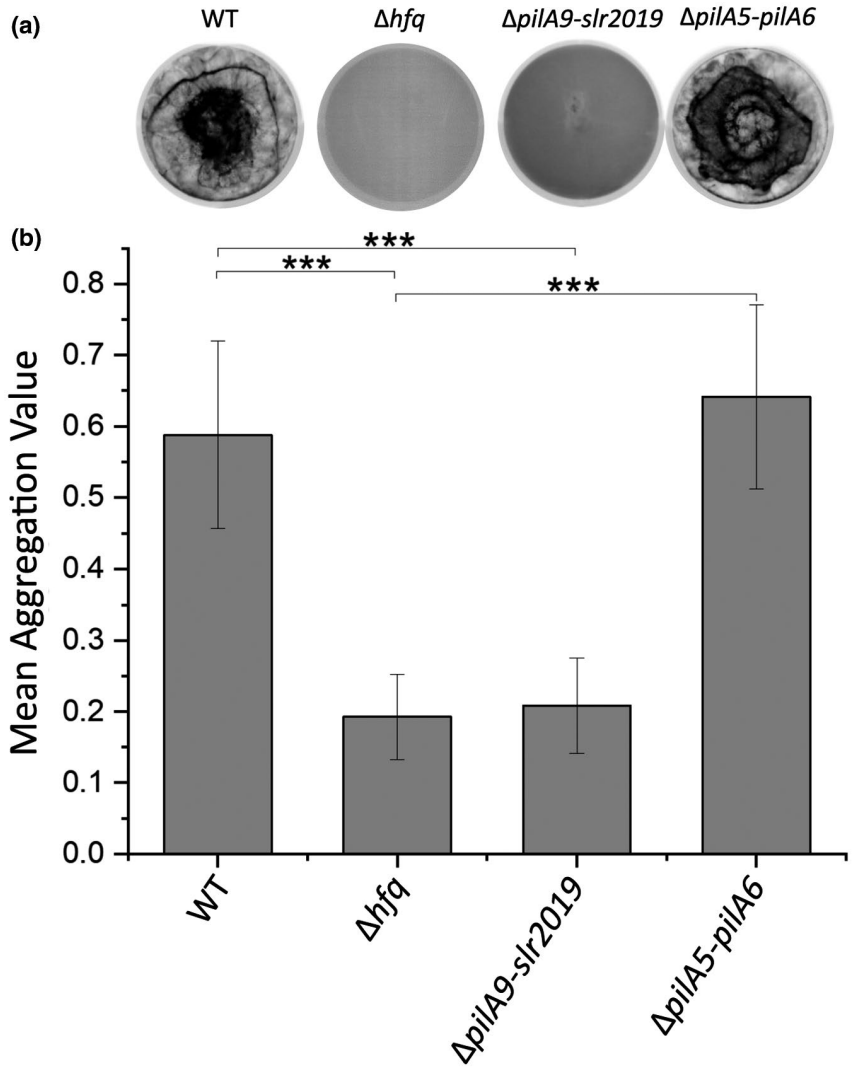

FIGURE 2 Involvement of minor pilins in flocculation. (a) Representative flocculation assays for WT *Synechocystis* cells and deletion mutants Δ*hfq*, Δ*pilA9-slr2019*, and Δ*pilA5-pilA6*. Chlorophyll fluorescence is shown in inverted greyscale; thus, areas with more chlorophyll appear darker. (b) Mean aggregation values of WT ($n = 19$), Δ*pilA5-pilA6* ($n = 19$), Δ*hfq* ($n = 12$), and Δ*pilA9-slr2019* ($n = 7$). Three asterisks indicate statistical significance with p values ≤ .001, calculated via Student's t test

(Schuergers et al., 2014). For our study, we used the Δ*hfq* strain because inactivation of the *hfq* gene leads to non-motile and T4P lacking cells (Dienst et al., 2008).

To determine whether the attachment of T4P to surfaces and their dynamics is impaired in the Δ*pilA5-pilA6* and Δ*pilA9-slr2019* strains, we used fluorescent beads and monitored the retraction of the beads to the cell surface, as described by Nakane and Nishizaka (2017). To that end, a glass surface was coated with 4% collodion; thus, cells were not able to move, though they were still able to assemble and retract T4P. The bead assays suggest that the WT pili attach to nearby beads and transport them towards the cell (Figure 3a and Video S1). Interestingly, Δ*pilA9-slr2019* mutant cells were not able to adhere to the collodion surface. However, in some cases, single cells were trapped on the glass slide, but they were not able to attach to the beads (Figure 3b and Video S2). In contrast, Δ*pilA5-pilA6* mutant cells were able to retract beads towards the cell (Figure 3c and Video S3).

These results indicate that the lack of the *pilA9-slr2019* gene cluster causes a defect in T4P function related to motility and attachment to biotic and abiotic substances, whereas the minor pilins PilA5 and PilA6 are dispensable for these processes.

2.2 | Role of minor pilins in natural competence

T4P are also known to be important for natural competence (Piepenbrink, 2019; Schirmacher et al., 2020; Yoshihara et al., 2001). Therefore, we investigated the ability of the minor pilin mutants described above to be transformed by exogenous DNA. We used a plasmid that enables integration via homologous recombination of a streptomycin resistance cassette into the chromosomal region of the gene encoding the small RNA PsrR1 (Georg et al., 2014). The Δ*pilA9-slr2019* mutant strain was transformable with a transformation efficiency similar to that of the WT (Figure 4). The Δ*hfq* strain was employed as a negative control, as this strain is not transformable (Dienst et al., 2008). Notably, the Δ*pilA5-pilA6* mutant strain was not transformable (Figure 4). To discriminate the function of PilA5 and PilA6, we complemented the Δ*pilA5-pilA6* strain with plasmids for the expression of *pilA5*, *pilA6* or the whole *pilA5-pilA6* operon (Figure S1). To each coding sequence, the putative native promoter region (extending 450 bp upstream of the *pilA5* start codon) was fused. Though the standard deviations of transformation efficiency were very high in these experiments, it is clear that only in the strains that contained the *pilA5* gene, either the *pilA5* gene alone or

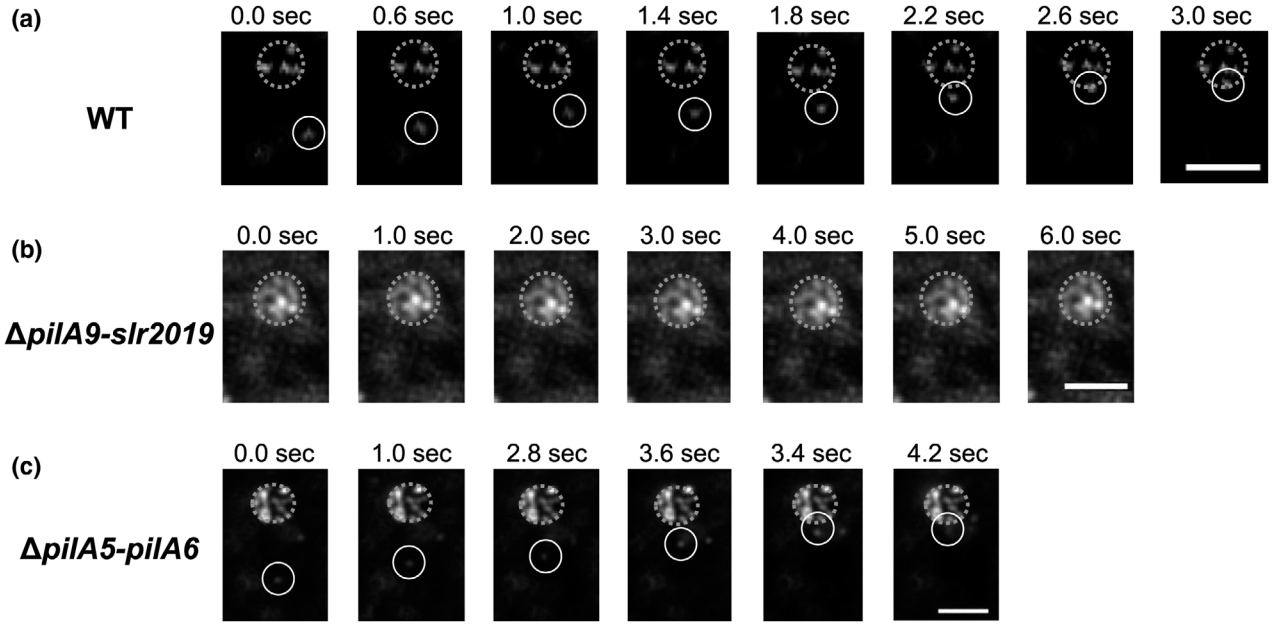

FIGURE 3 Pili can bind and retract fluorescent beads. Picture series of WT (a), Δ*pilA9-slr2019* (b), and Δ*pilA5-pilA6* (c) cells binding fluorescent beads in the medium. Cells are immobilized on a collodion surface and indicated by dotted circles. Representative pilus-bound beads are indicated by solid line circles. Scale bars: 3 μm. Original videos can be found in the supplementary data (Videos S1–S3)

in combination with *pilA6*, streptomycin-resistant clones were detectable (Figure 4). Exconjugants containing the plasmid with only the *pilA6* gene were not transformable (Figure 4), and Northern Blot analysis verified that *pilA6* was transcribed in this strain (Figure S2). Therefore, we conclude that the minor pilin PilA5 is essential for DNA uptake.

2.3 | Minor pilin mutants assemble thick pili on the surface of *Synechocystis* cells

To determine whether the lack of specific pilus functions is related to a defect in pilus assembly, we examined negative stained cells by transmission electron microscopy (TEM). Notably, we were able to detect thick pili in the WT and in the two minor pilin operon deletion mutants (Figure 5). In all strains, we measured a diameter of the thick pili between 5.5 and 9 nm (Figure S3), which is comparable to the 6 to 8 nm described by Bhaya et al. (2000). This result suggests that all minor pilin deletion mutants can assemble T4P. Moreover, immunodetection and quantification of the major pilin PilA1 in sheared pili fractions indicates, that piliation of Δ*pilA9-slr2019*, Δ*pilA5-pilA6* and Δ*pilA5-pilA6* complementation mutants is comparable to the WT (Figure 6).

In addition to T4P, *Synechocystis* also possesses thin pili with unknown molecular composition and function. All mutant strains analyzed in our study were shown to produce these thin filaments (Figure 5). Therefore, the minor pilins PilA5, PilA6, PilA9, PilA10 and PilA11 and proteins Slr2018 and Slr2019 are not involved in general formation of thin or thick pili. Notably, with our improved imaging procedure, we could also visualize thin pili on the Δ*hfq* strain (Figure 5f). This is in contrast to previous observations by Dienst et al. (2008), which described the mutant nonpiliated.

In summary, minor pilin deletion mutants assemble thick pili, and the presence of thin pili was not impaired in any of the constructed mutants. Therefore, loss of motility and flocculation in Δ*pilA9-slr2019* and impaired natural competence in Δ*pilA5-pilA6* did not correlate with loss of T4P or thin pili.

2.4 | Transcriptional changes in response to surface acclimation

Minor pilins are involved in attachment and surface motility. Therefore, we attempted to determine if their transcription is regulated upon surface contact and whether *Synechocystis* is able to respond to surface contact in general. In *Pseudomonas*, mechanosensing of a surface with T4P leads to upregulation of a cAMP-dependent operon with significant transcriptional changes within 3 hr of surface contact (Persat et al., 2015). To evaluate the acclimation capacity of the slower growing *Synechocystis*, researchers usually analyze gene expression changes within 1 to 24 hr after transfer to new conditions (Hernández-Prieto et al., 2016). Therefore, we analyzed genome-wide transcriptional changes between *Synechocystis* planktonic cell cultures and cells on a surface (sessile culture) after 4 and 8 hr of surface incubation. We employed a microarray design that enables identification of all coding and non-coding RNA transcripts identified by previous transcriptomic studies (Klotz et al., 2016; Kopf et al., 2014; Mitschke et al., 2011). We defined a $\log_2$ fold change (FC) $\geq |-0.8|$ and an adjusted p value $< .05$ as the threshold for a transcriptional change (comparable to Wallner et al., 2020). Based on

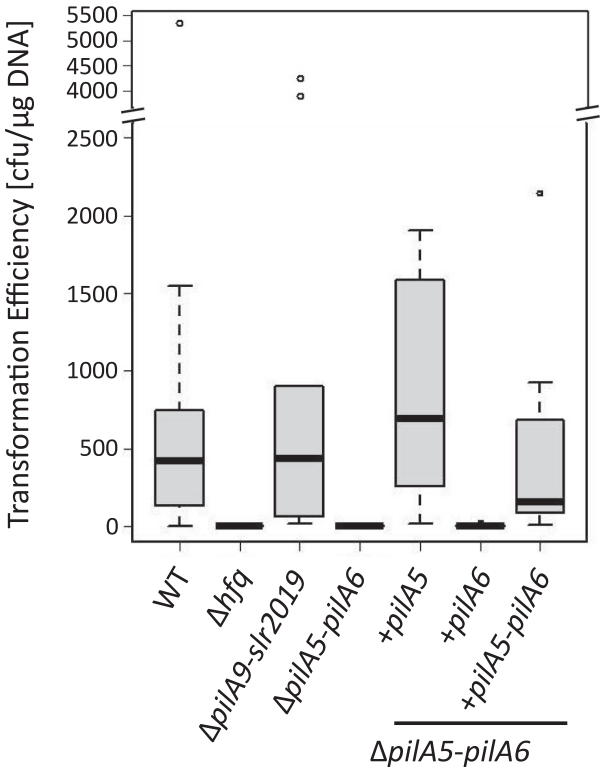

FIGURE 4 Transformation efficiency of different minor pilin mutants. The transformation efficiency of WT ($n = 16$), Δ*hfq* ($n = 13$), Δ*pilA9-slr2019* ($n = 9$), Δ*pilA5-pilA6* ($n = 16$) and Δ*pilA5-pilA6*/+*pilA5* ($n = 7$), Δ*pilA5-pilA6*/+*pilA6* ($n = 7$) *and* Δ*pilA5-pilA6*/+*pilA5-pilA6* ($n = 7$) cells was determined. The deletion mutant Δ*hfq* lacking T4P was used as a negative control. Transformations were performed with different amounts of DNA ranging from 500 ng to 1 µg

these criteria, the transcript accumulation of 122 genes changed after surface acclimation (Figure S4, Tables 1 and 2). As depicted on the heatmap in green (Figure 7) and in the volcano plot in blue (Figure S4), genes on the 120 kbp pSYSM plasmid showed the highest differential transcription upon surface contact. The transcript levels of 10 genes on the pSYSM plasmid were downregulated, and three were upregulated, together representing approximately 10% of the 132 annotated genes on this plasmid (Kaneko et al., 2003). One of the most upregulated TU at both time points after transfer of the cells to a surface is located on the pSYSM plasmid and encodes the two hypothetical proteins Slr5087 and Slr5088.

Notably, the mRNA of the minor pilin gene operon *pilA5-pilA6* accumulated under sessile conditions, whereas the genes *pilA9*, *pilA10*, *pilA11* and *slr2018* showed higher transcript accumulation during the planktonic lifestyle. The downstream *slr2019* open reading frame does not appear to be differentially transcribed based on our significance criteria, implying that this gene may not be part of *TU763* or that there is posttranscriptional gene regulation.

Interestingly, the most strongly upregulated mRNA after 4 hr (but not after 8 hr) of incubation on an agar plate encodes the high affinity bicarbonate uptake system SbtA (Shibata et al., 2002). Further genes known to accumulate under inorganic carbon (C_i) limitation (e.g., *sll1594*, encoding the transcriptional regulator NdhR, and the hypothetical genes *slr1634*, *slr1770*, *slr0226*, *slr0006*, and *slr2006* [Orf et al., 2016]) showed the same response in our microarray study, implying that cells experience a short term CO_2 limitation during surface acclimation. Other genes of components of the inducible bicarbonate/CO_2 uptake systems (e.g., *ndhF3/D3*, *cmp*, and *cupA*) show a similar altered transcription, however they did not meet our significance criteria.

Furthermore, most upregulated genes 4 hr after transfer to agar plates are *sll0783*, which is involved in polyhydroxybutyrate synthesis (Schlebusch & Forchhammer, 2010), and *slr1667*, a component of a putative chaperone usher pathway (Schuergers & Wilde, 2015) (Table 1). Loci that show increasing transcript accumulation in sessile cultures over the 8-hr acclimation period are either located on pSYSM or are involved in nitrate or cyanate metabolic processes (e.g., *nrtAB* and *cynS*) or pilus function (such as the minor pilin genes *pilA5* and *pilA6*) (Table 1). A further operon with a similar transcription profile is *slr1593/slr1594*, which encodes an EAL domain protein and a CheY-like response regulator with unknown functions (Table 1).

The most downregulated genes in response to surface exposure are again transcribed from the pSYSM plasmid (Table 2). Other genes that show higher transcription in planktonic cultures than in sessile cultures encode sulfate and phosphate transport systems, proteins related to transcription/translation and hypothetical proteins (Figure 7; Table 2). The transcription levels of some genes remain low or decrease further in surface-grown cells after 8 hr. Among them are the plasmid gene *slr5055*, encoding a glycosyltransferase of a newly identified EPS synthesis cluster (Maeda et al., 2021) and the polycistronic mRNA for minor pilins (*pilA9-pilA11*). These data were verified by Northern blot hybridizations (Figure S5) which also show that at least the mRNA which hybridized to the *pilA9* probe exhibited lower signal intensity under sessile conditions already at 10 min and 1 hr after surface contact (Figure S5b).

In addition to the transcriptional changes in mRNAs, we detected 16 non-coding RNAs (ncRNA) which were upregulated after 4 hr on surface (e.g., PmgR1 [*ncr0700*] and IsaR1 [*ncl1600*]) and 6 ncRNAs which were downregulated under sessile conditions (e.g., SyR6 [*ncl0880*] and CsiR1 [*ncr038*]; Supplementary Data Table). These ncRNAs are known to be involved in acclimation to nutrient starvation (Giner-Lamia et al., 2017; Kopf et al., 2014; De Porcellinis et al., 2016; Rübsam et al., 2018).

2.5 | Identification of putative new minor pilins of *Synechocystis*

Our microarray analysis identified several chromosomal genes that showed a comparably stable transcriptional change during the 8 hr of surface acclimation. Among these genes, *slr0226*, as well as *pilA5* and *pilA6*, exhibited increased transcription under sessile conditions, whereas *slr0442* and the *pilA9-pilA11* transcripts accumulate in planktonic cultures over the whole sampling time (Tables 1 and 2).

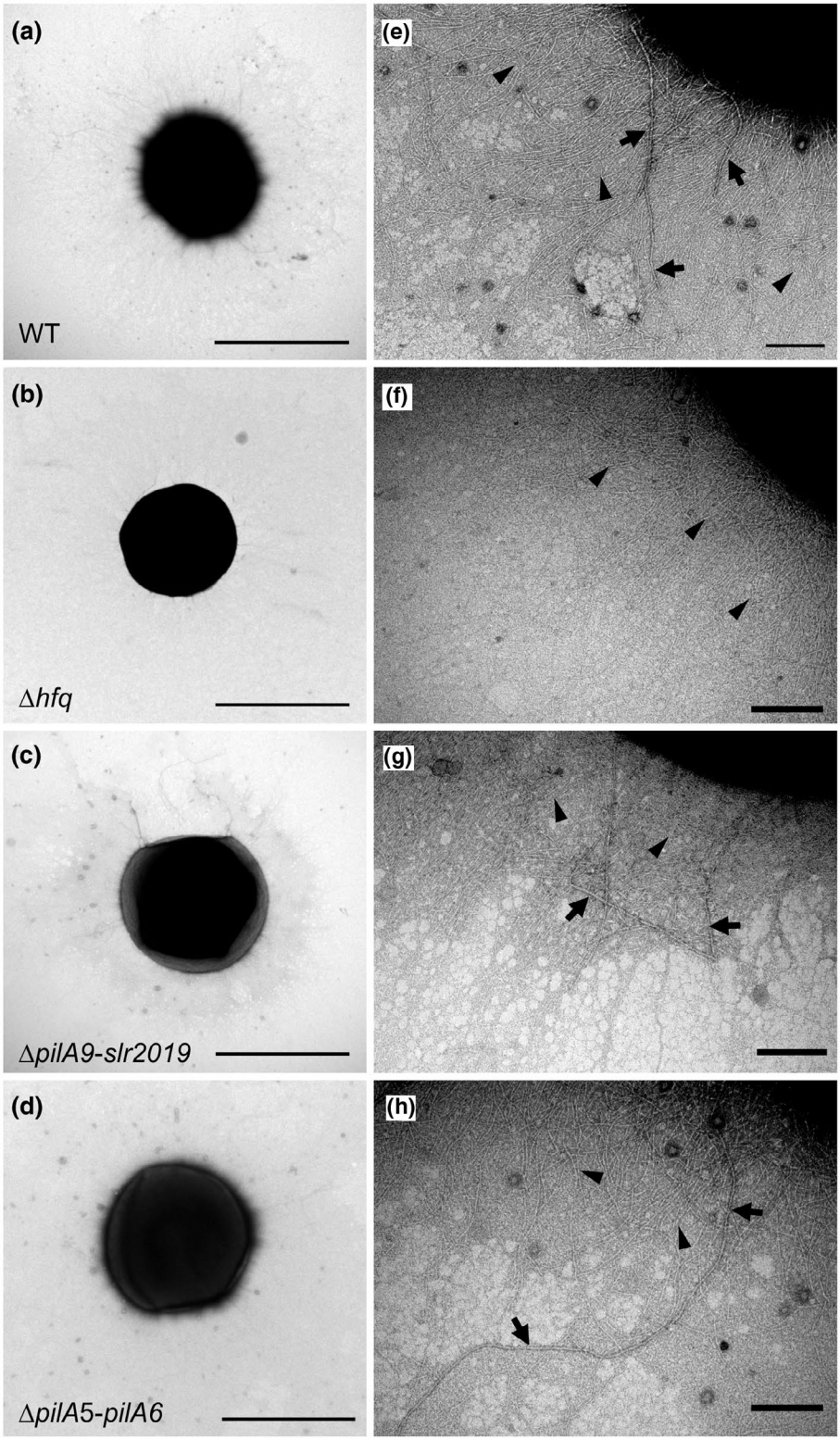

FIGURE 5 Electron micrographs of different negatively stained *Synechocystis* strains. WT (a, e), T4P lacking deletion mutant Δ*hfq* (b, f) and deletion mutants Δ*pilA9-slr2019* (c, g) and Δ*pilA5-pilA6* (d, h) were negatively stained with 1% uranyl acetate. Whole cells are depicted in (a-d) (scale bar 2 μm) and ultrastructural details of pili are shown in (e–h) (scale bar 200 nm) with distinct types of thick pili (black arrow) and thin pili (arrowhead)

Notably, these transcripts were also coregulated in other transcriptomic studies (Dienst et al., 2008; Kizawa et al., 2016; Wallner et al., 2020; Yoshimura, Yanagisawa, et al., 2002, see also discussion).

Synteny analysis using the tool FlaGs (Saha et al., 2020, Table S6) demonstrated that in many cyanobacteria, a hypothetical protein (Figure S6; Table S1) is encoded directly upstream or downstream of

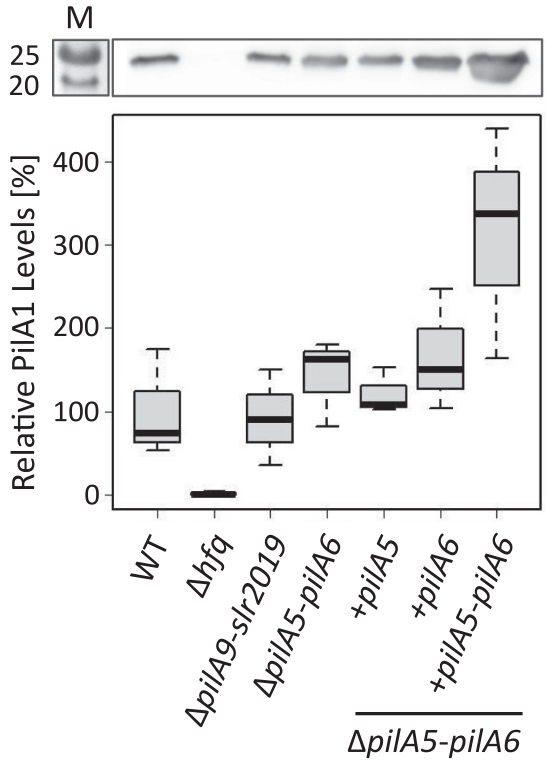

FIGURE 6 PilA1 quantification of different minor pilin mutants. Representative Western Blot analysis of sheared pili fractions of the WT, the Δ*hfq*, the Δ*pilA9-slr2019*, the Δ*pilA5-pilA6* deletion mutants, as well as the Δ*pilA5-pilA6*/+*pilA5*, Δ*pilA5-pilA6*/+*pilA6* and Δ*pilA5-pilA6*/+*pilA5-pilA6* reinsertion mutants with an antibody against the major pilin PilA1 and relative PilA1 levels to the mean WT PilA1 level ($n = 3$). M—BlueStar Plus Prestained Protein Marker (NIPPON Genetics, Europe)

pilA5 homologues from other cyanobacteria (Figure S6a, Table S1). Such a gene was not found in proximity to *pilA5* in *Synechocystis*. However, using a protein sequence of this hypothetical gene (WP_008273982.1) as query, we identified in PHI-BLAST searches three *Synechocystis* genes with e-values less than 6×10^{-11}, which are *slr0226*, *slr0442* and *sll1268*. Further analysis showed that pilins are often encoded in genetic proximity to the homologues of these three genes (Figure S6b-d, Table S1). Slr0226, Slr0442, and Sll1268 are annotated as hypothetical proteins, but all contain a conserved PilX-N-terminal domain (HHsearch probability > 95%; Figure S7). PilX is a minor pilin from *Pseudomonas* that is essential for motility and is implicated as a key promoter of pilus assembly (Giltner et al., 2010).

In order to reveal a possible function of these putative minor pilin genes, we created knock-out mutants of the *pilX*-like genes *slr0226* (*pilX1*), *slr0442* (*pilX2*) and *sll1268* (*pilX3*) (Figure S8). First, we checked the piliation of the *Synechocystis pilX* mutant strains with TEM (Figure 8). Clearly, all three *pilX* deletion mutants present thick and thin pili on their surface (Figure 8). Phototaxis experiments revealed that the mutant strains Δ*pilX1* and Δ*pilX3* are motile, whereas the Δ*pilX2* deletion mutant showed highly reduced motility (Figure 9a). Notably, *pilX2* shows the same transcription pattern as *pilA9-slr2019* in our transcriptomic analysis. Further, we tested the newly created Δ*pilX* deletion mutants for flocculation and discovered that none of the *pilX* deletion mutants was able to flocculate (Figure 9b). A transformation test, however, revealed that all *pilX* mutants are transformable (Figure 9c). Thus, the *pilX2* and *pilA9-slr2019* mutants have a similar phenotype, whereas Δ*pilX1* and Δ*pilX3* show a new combination of phenotypic characteristics. They are not able to form flocs, though they are still motile and transformable. A summary of the phenotypes of minor pilin mutants analyzed in our study in comparison to the WT and a Δ*pilA1* strain is given in Table 3.

2.6 | Possible functions of pSYSM-encoded genes

Some of the most differentially transcribed genes between planktonic and surface-grown cells were encoded on the pSYSM plasmid (Tables 1 and 2). Ten genes with significantly lower transcript accumulation upon surface contact belong to a gene cluster consisting of 19 genes involved in biosynthesis of the recently identified sulphated extracellular polysaccharide synechan. This polysaccharide was shown to be essential for aggregate formation in planktonic cultures (Maeda et al., 2021).

The three genes with upregulated transcription in sessile lifestyle could not be classified into a specific biological process (*slr5087*, *slr5088*, *slr5037*; Table 1). As the genes *slr5087* and *slr5088* showed the highest upregulation upon surface contact, we sought to test the phenotypes of their respective deletion mutant, Δ*slr5087-5088* (Figure S9). We performed phototaxis experiments and flocculation assays. However, we could not detect any difference between the mutant and the WT (Figure S9). Notably, phototactic movement of this mutants and the *pilA5-pilA6* minor pilin mutants was reduced compared to the WT. We often observe this phenomenon for different mutants which might be due to secondary effects of the antibiotic resistance cassette insertion. We could show that the complementation of the *pilA5-pilA6* deletion restored natural competence but also resulted in retarded movement (Figure S10). These differences are difficult to quantify and may vary between different experiments. Therefore, based on macroscopic motility on plates, we do not expect a possible minor involvement of these genes in motility, though we are not able to completely exclude such effects at the moment.

2.7 | Concentrations of the second messenger nucleotides cAMP and c-di-GMP change upon acclimation to a surface

Previously, it was shown that the two sets of minor pilins analyzed in this study are differentially transcribed in a c-di-GMP-dependent manner (Wallner et al., 2020). Therefore, we analyzed the intracellular accumulation of c-di-GMP upon the transfer of cells from a planktonic lifestyle to a surface. Cells were treated as for RNA sampling. We were not able to detect significant changes (p values ≤ .05) in the cellular c-di-GMP level after planktonic cells were incubated for 4 and 8 hr

TABLE 1 Upregulated genes in sessile conditions compared to planktonic conditions

Locus tag	Location	Gene name	Functional annotation	log_2 FC sessile—planktonic 4 hr	log_2 FC sessile—planktonic 8 hr
slr1512	chr	*sbtA*	Sodium-dependent bicarbonate transporter	3.674	0.132
slr0376	chr	*slr0376*	Hypothetical protein	3.144	1.529
sll0783	chr	*sll0783*	Unknown protein	2.260	2.137
slr1667	chr	*cccS*	Hypothetical protein, target of SyCRP1	2.171	1.256
slr5087	pSYSM	*slr5087*	Hypothetical protein	2.052	3.516
slr0373	chr	*slr0373*	Hypothetical protein	1.985	0.533
slr0374	chr	*slr0374*	Hypothetical protein	1.955	0.635
slr1634	chr	*slr1634*	Hypothetical protein	1.924	0.219
slr1770	chr	*slr1770*	Hypothetical protein	1.905	1.415
slr0226	chr	*slr0226*	Potential minor pilin[a], PilX N-terminal domain containing protein	1.796	1.399
sll1594	chr	*ndhR*	NAD(P)H dehydrogenase transcriptional regulator, LysR family protein	1.717	0.580
slr0006	chr	*slr0006*	Unknown	1.635	0.356
slr2006	chr	*slr2006*	Hypothetical protein	1.612	0.606
slr5088	pSYSM	*slr5088*	Probable short-chain dehydrogenase	1.558	3.096
sll0784	chr	*sll0784*	Nitrilase	1.398	0.693
sll0944	chr	*sll0944*	Hypothetical protein	1.216	1.196
slr1928	chr	*pilA5*	Minor pilin, involved in competence[a]	1.195	1.331
sll1080	chr	*sll1080*	ABC transport system substrate-binding protein	1.069	0.380
slr0967	chr	*slr0967*	Hypothetical protein	0.979	0.917
sll1086	chr	*sll1086*	Unknown protein	0.970	0.461
sll1891	chr	*sll1891*	Unknown protein	0.960	0.530
slr0007	chr	*slr0007*	Probable sugar-phosphate nucleotidyltransferase	0.957	0.279
slr1594	chr	*slr1594*	Two-component response regulator PatA subfamily	0.944	1.234
slr1593	chr	*slr1593*	Hypothetical protein (EAL domain)	0.921	1.233
slr1811	chr	*slr1811*	Hypothetical protein	0.908	0.720
slr1095	chr	*slr1095*	Hypothetical protein	0.901	0.718
sll0168	chr	*sll0168*	Hypothetical protein	0.876	0.861
slr1612	chr	*slr1612*	Hypothetical protein	0.856	0.762
slr5037	pSYSM	*slr5037*	Hypothetical protein	0.854	0.963
slr1674	chr	*slr1674*	Hypothetical protein	0.849	0.852
slr0898	chr	*nirA*	Ferredoxin-nitrite reductase	0.844	1.847
slr0288	chr	*glnN*	Glutamate-ammonia ligase	0.843	0.821
ssr2062	chr	*ssr2062*	Hypothetical protein	0.843	0.393
slr2007	chr	*ndhD5*	NADH dehydrogenase subunit 4	0.840	0.270
sll0785	chr	*sll0785*	Unknown protein	0.803	0.336
sll1079	chr	*hypB*	Putative hydrogenase expression/formation protein HypB	0.802	0.203
slr1739	chr	*psb28*	Photosystem II reaction center Psb28 protein	0.801	0.639
sll1450	chr	*nrtA*	Nitrate/nitrite binding protein	0.593	1.453
sll1451	chr	*nrtB*	Nitrate import permease protein	0.369	1.385
slr0899	chr	*cynS*	Cyanate hydratase	0.281	1.262

(Continues)

TABLE 1 (Continued)

Locus tag	Location	Gene name	Functional annotation	log_2 FC sessile—planktonic 4 hr	log_2 FC sessile—planktonic 8 hr
ssl3446	chr	*ssl3446*	Hypothetical protein	0.569	1.150
sll0661	chr	*ycf35*	Hypothetical protein Ycf35	0.467	1.053
slr1929	chr	*pilA6*	Minor pilin	0.779	0.892
slr1915	chr	*slr1915*	Hypothetical protein	0.647	0.875
slr0299	chr	*slr0299*	Hypothetical protein	0.748	0.800

Note: Listed are differentially transcribed genes after growth for 4 or 8 hr either under planktonic or sessile conditions. Shown are only protein encoding genes. Hits underneath the horizontal solid line indicate genes that were only considered significant after 8 hr. Fold changes (FC) were considered significant with a log_2 FC ≤−0.8 or ≥+0.8 and adjusted p value < .05. Adjusted p values were calculated using the Benjamini-Hochberg test. Functional annotation was derived from the CyanoBase and UniProt databases (Jan 2020).

Abbreviation: chr, chromosome.

[a]Shown in this study.

on an agar plate (Figure 10). Therefore, an altered c-di-GMP content appears not to be directly responsible for the transcriptional changes detected in the microarray analysis at these time points. However, elevated c-di-GMP concentrations were detected after 10 min and 1 hr under sessile conditions (Figure 10). This result suggests a very fast response of the second messenger to surface contact. Comparison of c-di-GMP-dependent transcriptional changes (Wallner et al., 2020) and altered gene transcript levels upon surface contact indicates only a small overlap or even opposite changes between these two analyses (see Section 3). Further, we revealed a rapid response of cAMP accumulation upon surface contact and an approximately 3.6-fold elevated cAMP level after 4 hr on agar compared to planktonically grown cells.

Taken together, we detected a very rapid increasing response of the second messengers cAMP and c-di-GMP within the first minutes after surface contact. However, the intracellular second messenger levels after 4 and 8 hr were almost indistinguishable between sessile and planktonic cells.

3 | DISCUSSION

3.1 | Response of *Synechocystis* to surface contact

Our transcriptome analyses demonstrated that minor pilin genes are targeted by a putative surface response system in *Synechocystis* cells. Some of the minor pilin transcripts accumulated in surface-grown cells, while others accumulated in planktonic culture. The *pilX1* mRNA accumulates under sessile conditions along with the mRNA encoding *pilA5* and *pilA6*. In contrast, the transcription of *pilX2* and *pilA9-slr2019* was downregulated under sessile conditions (Table 1). The accumulation of these two transcripts which encode five different minor pilins was also reduced in *Synechocystis* mutants lacking the homolog of the RNA chaperone Hfq (Dienst et al., 2008), the transcription factors LexA (Kizawa et al., 2016) and SyCRP1 (Yoshimura, Yoshihara, et al., 2002) and the blue-light inducible diguanylate cyclase Cph2 (Wallner et al., 2020), whereas the transcripts of *pilX1* and *pilA5-pilA6* both accumulated to higher level in the Δ*cph2* strain when compared to the WT. Thus, in *Synechocystis*, specific sets of minor pilins are coregulated, suggesting that they belong to the same regulon and function in the same process or under the same condition. Notably, changes in transcript accumulation can result from transcription control via transcription factors as well as from post-transcriptional events, such as transcript stability and/or processing. We are not able to discriminate between these regulatory principles in our analysis, though the overlap in transcriptional changes in different transcription factor mutants and *hfq* suggest a control of RNA accumulation on different levels.

Wallner et al. (2020) showed that the minor pilins were a major target of c-di-GMP-dependent signalling. In summary, eleven out of 17 genes that are known to be regulated by c-di-GMP under blue-light illumination (Wallner et al., 2020) also responded to surface contact in our analysis. Taken together, we identified 122 surface-responding genes in our microarray study, which suggested a considerably larger response to that signal compared to c-di-GMP-based regulation. However, the transcriptional changes between surface versus planktonic growth in the current study and high c-di-GMP versus low c-di-GMP conditions (Wallner et al., 2020) do not support the idea that this second messenger is directly or solely involved in controlling gene transcription in response to a surface. For example, the *pilA9-slr2019* operon was downregulated during surface incubation (Table 2), whereas a high c-di-GMP content has been observed to lead to upregulation of this mRNA (Wallner et al., 2020). Laventie et al. (2019) showed for *Pseudomonas* that the c-di-GMP concentration increased within seconds upon surface contact, thereby leading to pilus assembly and enhanced surface attachment. We were also able to measure an increase in c-di-GMP and cAMP levels at shorter time points, such as 10 min or 1 hr after transfer to sessile conditions, suggesting that there is a short-term surface response in *Synechocystis* involving second messenger molecules. However, whether and how such a signal triggers some of the specific gene expression changes we observed after 4 and 8 hr of surface acclimation needs to be studied in the future. At least for *pilA9* such a short response on transcriptional level was detected (Figure S5b), but a more comprehensive analysis on the timing of acclimation

TABLE 2 Downregulated genes in sessile conditions compared to planktonic conditions

Locus tag	Location	Gene name	Functional annotation	log_2 FC sessile—planktonic 4 hr	log_2 FC sessile—planktonic 8 hr
slr5055	pSYSM	*slr5055*	Similar to UDP-N-acetyl-D-mannosaminuronic acid transferase	−5.005	−5.537
sll5057	pSYSM	*sll5057*	Probable glycosyltransferase	−4.806	−5.113
slr1452	chr	*sbpA*	Sulfate-binding protein	−3.650	−2.389
sll5046	pSYSM	*sll5046*	Unknown protein	−3.504	−3.742
sll5044	pSYSM	*sll5044*	Unknown protein	−3.008	−3.132
slr0364	chr	*slr0364*	Hypothetical protein	−2.803	−3.522
slr1453	chr	*cysT*	Sulfate transport system permease protein	−2.670	−1.626
ssr2439	chr	*ssr2439*	Hypothetical protein	−2.633	−1.574
slr1454	chr	*cysW*	Sulfate transport system permease protein	−2.476	−1.456
slr5056	pSYSM	*slr5056*	Probable glycosyltransferase	−2.331	−2.544
slr0366	chr	*slr0366*	Unknown protein	−2.273	−2.746
sll5043	pSYSM	*sll5043*	Probable glycosyltransferase	−2.254	−2.541
ssr2848	chr	*ssr2848*	Unknown protein	−2.025	−2.316
sll5042	pSYSM	*sll5042*	Probable sulfotransferase	−1.844	−2.070
slr5053	pSYSM	*slr5053*	Unknown protein	−1.752	−1.983
ssl5045	pSYSM	*ssl5045*	Unknown protein	−1.713	−1.802
slr1455	chr	*cysA*	Sulfate/thiosulfate import ATP-binding protein	−1.697	−0.804
slr0442	chr	*slr0442*	Potential minor pilin[a] PilX N-terminal domain containing protein	−1.293	−1.267
sll1745	chr	*rplJ*	50S ribosomal protein L10	−1.243	−1.045
sll1808	chr	*rplE*	50S ribosomal protein L5	−1.182	−1.039
sll1746	chr	*rplL*	50S ribosomal protein L12	−1.164	−0.829
sll1804	chr	*rpsC*	30S ribosomal protein S3	−1.155	−0.885
sll1813	chr	*rplO*	50S ribosomal protein L15	−1.151	−0.963
sll1801	chr	*rplW*	50S ribosomal protein L23	−1.148	−0.918
sll1809	chr	*rpsH*	30S ribosomal protein S8	−1.147	−0.963
sll1744	chr	*rplA*	50S ribosomal protein L1	−1.121	−0.725
sll0680	chr	*pstS*	Phosphate-binding protein	−1.120	−0.808
sll1803	chr	*rplV*	50S ribosomal protein L22	−1.116	−1.005
sll1810	chr	*rplF*	50S ribosomal protein L6	−1.099	−0.894
sll1743	chr	*rplK*	50S ribosomal protein L11	−1.064	−0.615
sll1811	chr	*rplR*	50S ribosomal protein L18	−1.061	−0.839
sll1799	chr	*rplC*	50S ribosomal protein L3	−1.060	−0.691
sll1806	chr	*rplN*	50S ribosomal protein L14	−1.056	−0.815
sll1800	chr	*rplD*	50S ribosomal protein L4	−1.051	−0.806
sll1807	chr	*rplX*	50S ribosomal protein L24	−1.045	−0.832
sll1815	chr	*adk1*	Adenylate kinase 1	−1.044	−0.751
sll1802	chr	*rplB*	50S ribosomal protein L2	−1.039	−0.739
ssl3432	chr	*rpsS*	30S ribosomal protein S19	−1.017	−0.621
sll1805	chr	*rplP*	50S ribosomal protein L16	−0.989	−0.798
slr0423	chr	*rlpA*	Probable endolytic peptidoglycan transglycosylase	−0.984	−0.234
slr1456	chr	*pilA4*	Minor pilin	−0.984	−0.476
sll0681	chr	*pstC*	Phosphate transport system permease protein	−0.961	−0.742
sll1812	chr	*rpsE*	30S ribosomal protein S5	−0.958	−0.741

(Continues)

TABLE 2 (Continued)

Locus tag	Location	Gene name	Functional annotation	log_2 FC sessile—planktonic 4 hr	log_2 FC sessile—planktonic 8 hr
sll1101	chr	*rpsJ*	30S ribosomal protein S10	−0.950	−1.067
slr1259	chr	*slr1259*	Hypothetical protein	−0.926	−1.566
ssl3437	chr	*rpsQ*	30S ribosomal protein S17	−0.920	−0.702
sll0262	chr	*des6*	acyl-CoA 6-desaturase	−0.908	−0.621
sll0263	chr	*sll0263*	Unknown protein	−0.901	−0.647
sll1818	chr	*proA*	DNA-directed RNA polymerase subunit alpha	−0.889	−0.649
slr2015	chr	*pilA9*	Minor pilin	−0.888	−0.934
ssl3436	chr	*rpmC*	50S ribosomal protein L29	−0.884	−0.682
slr2016	chr	*pilA10*	minor pilin	−0.879	−0.883
sll1260	chr	*rpsB*	30S ribosomal protein S2	−0.869	−0.590
slr2017	chr	*pilA11*	minor pilin	−0.847	−0.808
sll1096	chr	*rpsL*	30S ribosomal protein S12	−0.842	−0.556
sll1097	chr	*rpsG*	30S ribosomal protein S7	−0.841	−0.561
sll1323	chr	*atpG*	ATP synthase subunit b'	−0.839	−0.540
sll1261	chr	*tsf*	elongation factor	−0.835	−0.594
slr2018	chr	*slr2018*	Potential minor pilin	−0.828	−0.715
sll1951	chr	*sll1951*	S-layer protein	−0.819	−0.654
sll1742	chr	*nusG*	Transcription termination/antitermination protein	−0.818	−0.377
slr0676	chr	*cysC*	Adenylylsulfate kinase	−0.816	−0.224
sll1911	chr	*sll1911*	Hypothetical protein	−0.814	−0.523
sll1819	chr	*rplQ*	50S ribosomal protein L17	−0.807	−0.565
slr1260	chr	*slr1260*	Hypothetical protein	−0.781	−1.458
ssl1911	chr	*gifA*	Glutamine synthetase inactivating factor IF7	−0.396	−1.378
ssr0692	chr	*ssr0692*	Hypothetical protein	−0.502	−1.196
slr1204	chr	*htrA*	Protease	−0.638	−1.087
slr1535	chr	*slr1535*	Hypothetical protein	−0.265	−1.080
ssr1562	chr	*ssr1562*	Hypothetical protein	−0.532	−1.064
slr1261	chr	*slr1261*	Hypothetical protein	−0.521	−1.003
slr0749	chr	*chlL*	Light-independent protochlorophyllide reductase iron-sulfur ATP-binding protein	−0.246	−0.949
slr5054	pSYSM	*slr5054*	Probable glycosyltransferase	−0.714	−0.876
sll1009	chr	*frpC*	Iron-regulated protein	−0.591	−0.867
slr1262	chr	*slr1262*	Probable membrane transporter protein	−0.369	−0.854
slr0145	chr	*slr0145*	Unknown protein	0.352	−0.836
slr0750	chr	*chlN*	Light-independent protochlorophyllide reductase subunit N	−0.142	−0.811

Note: Listed are differentially transcribed genes after growth for 4 or 8 hr either under planktonic or sessile conditions. Shown are only protein encoding genes. Hits underneath the horizontal solid line indicate genes that were only considered significant after 8 hr. Fold changes (FC) were considered significant with a log_2 FC ≤−0.8 or ≥+0.8 and adjusted p value < .05. Adjusted p values were calculated using the Benjamini-Hochberg test. Functional annotation was derived from the CyanoBase and UniProt databases (Jan 2020).

Abbreviation: chr, chromosome.

[a]Shown in this study.

using fluorescent-based reporters for gene expression and second messenger levels would be required. The measured cellular c-di-GMP levels most probably do not reflect the exact situation in the cell, because this second messenger acts locally in the cell (without measurable changes in cellular c-di-GMP contents) as well as globally in complex signalling networks (Hengge, 2021). In addition, the two microarray studies are not directly comparable because of large differences in the growth conditions.

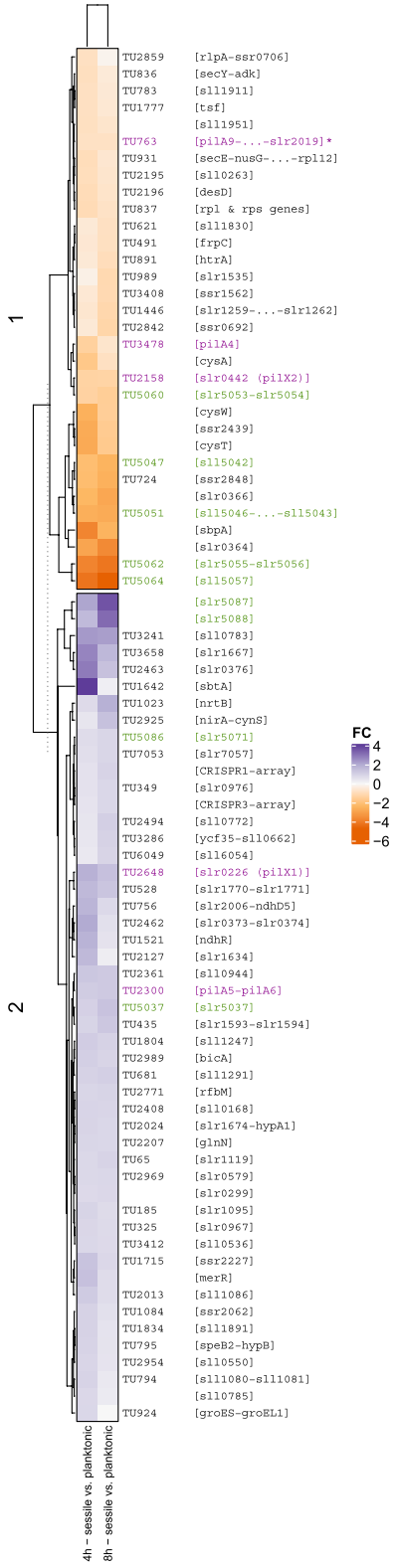

FIGURE 7 Transcription profiling of genes altered after 4 or 8 hr on sessile conditions compared to planktonic conditions. Heatmap of transcription levels of TUs with FC≥|0.8| and *p* value ≤ .05. Blue colour indicates higher transcription upon sessile conditions compared to planktonic conditions and orange colour indicates lower transcription. Lilac colour indicates minor pilin genes and green colour represents genes from the pSYSM plasmid. *TU763: $\log_2$ FC −0.781 (4 hr) and −0.786 (8 hr); with genes *pilA9-slr2018*: $\log_2$ FC −0.828 to −0.888 (4 hr) and *slr2019*: $\log_2$ FC −0.460 (4 hr) and 5′ UTR *TU763*: $\log_2$ FC −0.781 (4 hr)

The two CRP-like transcription factors SyCRP1 and SyCRP2 have been determined to be involved in second messenger signalling and are known to control the *pilX2* and the *pilA9-slr2019* operon (Song et al., 2018; Wallner et al., 2020; Yoshimura, Yoshihara, et al., 2002). Other studies predicted the binding of SyCRP1 to the promotor regions of *pilA9-2019*, *pilA5-pilA6*, *pilX2* and *pilX3* operons or genes. This was confirmed by in vitro binding studies for the *pilA5-pilA6*, *pilA9-2019*, *pilX2* and *pilX3* promoters (Omagari et al., 2008; Song et al., 2018). Together, these data suggest that cAMP is an important signal for the expression of minor pilins. It remains to be elucidated whether *Synechocystis* can sense a surface contact mechanically via its T4P. In *P. aeruginosa*, surface contact and shear stress generate tension in the pili leading to elevated levels of the second messengers cAMP and c-di-GMP (Gordon & Wang, 2019).

Further, we are not able to exclude that the cells also respond to the high culture density which is achieved on the surface of an agar plate. On one hand, high cell density affects light, nutrient and CO_2 availability, on the other hand, a high concentration of cells on a surface makes not only surface contact, but also a contact between the cells (e.g., via pili) more likely. In general, transcript accumulation of the minor pilin genes changes in response to several stress factors, e.g., the amount of both *pilA5-pilA6* and *pilX1* mRNAs is also upregulated under C_i conditions, stationary phase, heat stress and in the dark, whereas *pilA9-2019* and *pilX2* accumulation responds to low temperature and nitrogen limitation (Eisenhut et al., 2007; Kopf et al., 2014). This suggests a complex regulatory network on the level of transcript accumulation and/or stability for the minor pilin genes.

3.2 | Function of minor pilins in natural competence, motility, and flocculation

One of the mRNAs which accumulated in cells on a surface encodes the minor pilin PilA5 which is essential for natural competence. Within a biofilm it might be beneficial for the cell to take up DNA from adjacent cells, either as a nutrient or to gain new traits (Ibáñez de Aldecoa et al., 2017; Vorkapic et al., 2016). In freshwater environments, the concentration of extracellular DNA ranges from 1.75 to 7.7 µg/L (DeFlaun et al., 1986; Paul et al., 1989) which is an order of magnitude lower than in e. g in soil samples or in biofilms (Niemeyer & Gessler, 2002; Torsvik & Goksoyr, 1978). Thus, it seems more unlikely for planktonic, single cells to be in proximity of free-floating DNA in a water column; therefore, the demand for DNA uptake and PilA5 might be lower in a planktonic culture. In contrast to *pilA5*, the *pilA9-slr2019* operon is dispensable for natural competence but is involved in motility, bead attachment and flocculation. During floc formation, cells presumably bind to other cells or cellular components excreted by adjacent cells, such as T4P or EPS (Trunk et al., 2018). We assume that the *pilA9-slr2019* mutant can still retract its pili, as cells are still transformable. It seems that this mutant assembles pili that are not able to attach to a surface, other cells or beads.

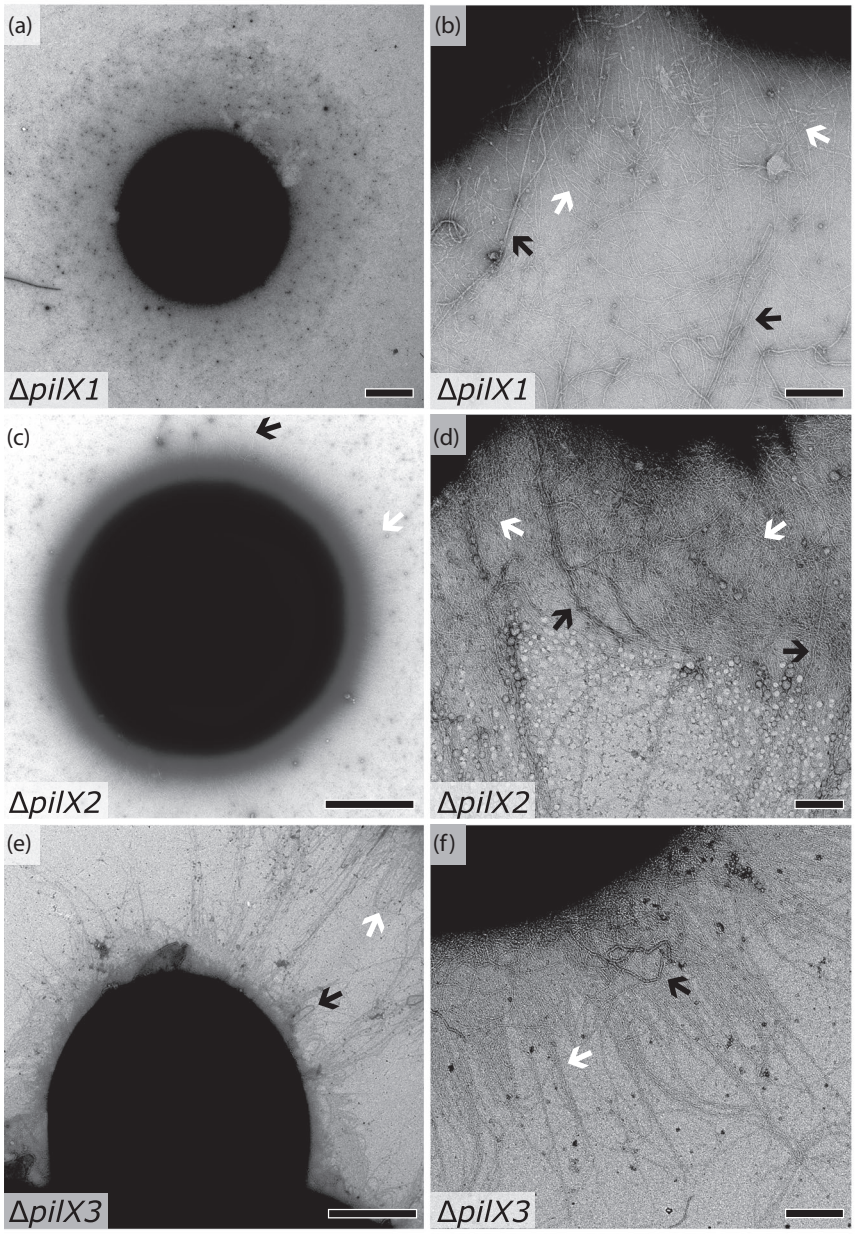

FIGURE 8 Electron microscopy images of the negatively stained three PilX deletion mutants. Cells were negatively stained with 2% uranyl acetate. Shown are whole cells (a, c, e) (scale bar 1 μm) and close ups (b, d, f) (scale bar 200 nm) of the Δ*pilX1* (a, b), the Δ*pilX2* (c, d) and Δ*pilX3* (e, f) deletion mutants. Black arrows depict representative thick pili, and white arrows representative thin pili

In *Myxococcus*, a complex of minor pilins (including a PilX homolog) is involved in priming pilus extension which is essential for assembling pili on the surface (Treuner-Lange et al., 2020). As we still detect thick pili on the surface of the analyzed mutants, we assume that the minor pilins and hypothetical proteins analyzed in our study are not essential for the assembly of a general priming complex. However, we hypothesize that the minor pilins can be part of a pilus structure. Indeed, the minor pilin PilA4 from *Synechocystis* was detected outside of the cell in a PilA1 dependent manner (Cengic et al., 2018) and PilA2 and PilA11 have been detected at the cell surface via affibodies against PilA2 and immunolabeling of PilA11 (Cengic et al., 2018; Hu et al., 2018). Notably, a mutant of the major pilin gene *pilA1* lacks thick pili on the surface but is still able to flocculate (Conradi et al., 2019). Therefore, it remains unclear whether the minor pilins which are involved in aggregation are part of the major pilus structure or can form a distinct pilus. Hu et al. (2018) reported that specific repression of *pilA11* mRNA via the naturally transcribed antisense RNA PilR leads to thinner and fewer pili, whereas depletion of PilR leads to overexpression of PilA11 and the opposite effects on pili. However, we were not able to measure significantly smaller diameters of the T4P in our mutant which lacks all minor pilins encoded in the Δ*pilA9-slr2019* operon (Figure S3). Generally, measuring precise diameters from TEM images is rather inaccurate and was not the aim of this study.

Whether the minor pilins analyzed in our study can be inserted into a pilus fiber remains unclear. Therefore, we attempted to model their structure. Due to poor inter- and intraspecies conservation of the amino acid sequences, we were only able to model PilA1, PilA4, PilA5, PilA6 and PilA10 with acceptable sequence coverage

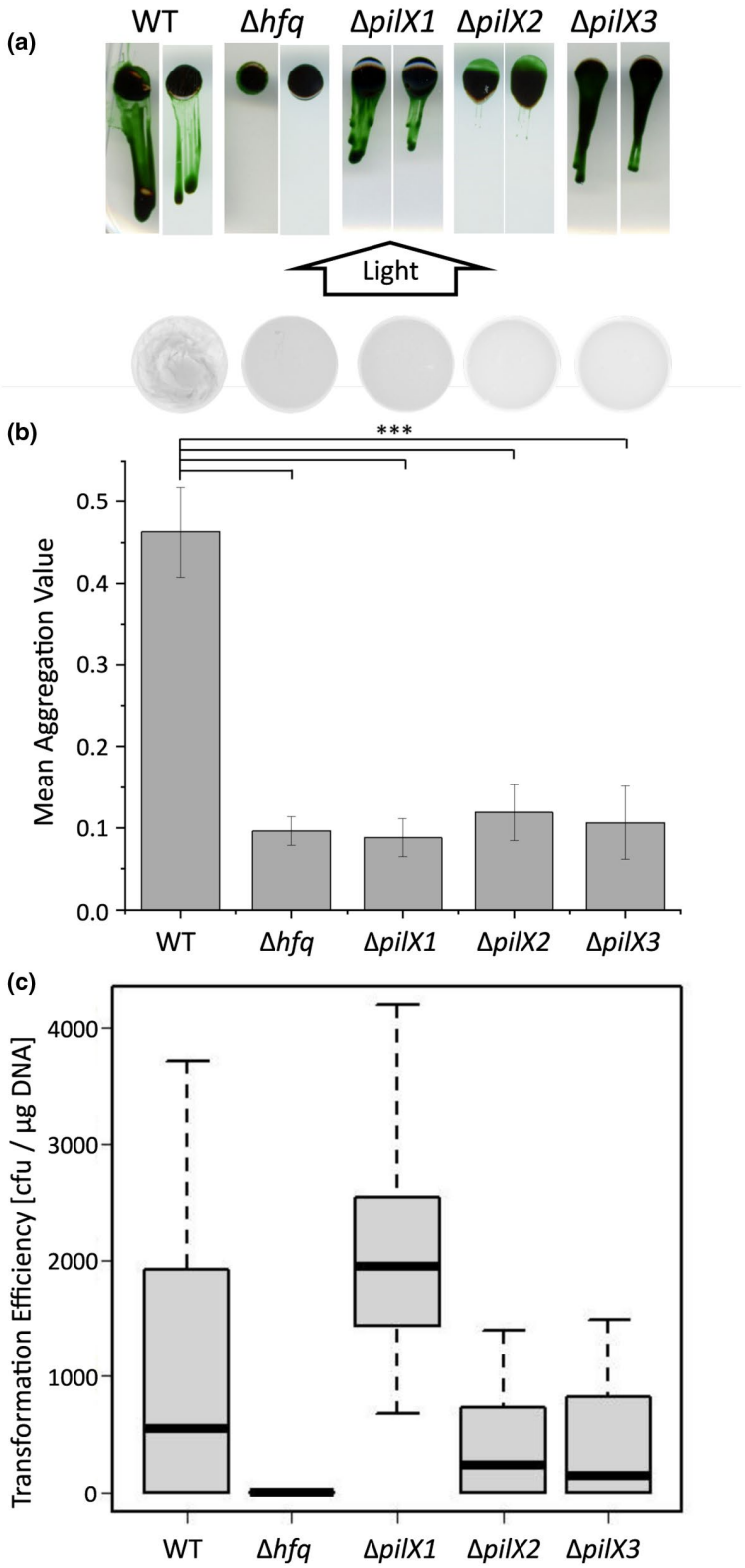

FIGURE 9 Phenotypes of the *pilX* deletion mutants. (a) Phototaxis assays of the Δ*pilX1*, Δ*pilX2* and Δ*pilX3* mutant strains of *Synechocystis*. Pictures were taken after 14 days of incubation with unidirectional white light. The Δ*hfq* strain was used as negative control. Shown are two independent clones of the respective *pilX* deletion mutants. (b) Flocculation assay of the *pilX* deletion strains. Chlorophyll fluorescence is shown in inverted greyscale in pictures at the top. The Δ*hfq* strain was used as negative control. Displayed are mean aggregation values of WT ($n = 12$), Δ*hfq* ($n = 12$), Δ*pilX1* ($n = 16$), Δ*pilX2* ($n = 16$) and Δ*pilX3* ($n = 16$). Three asterisks indicate statistical significance with p values ≤ .001, calculated via Student's t test. (c) Transformation efficiency of the *pilX* deletion mutants. The transformation efficiency of WT ($n = 8$), Δ*hfq* ($n = 6$), Δ*pilX1* ($n = 13$), Δ*pilX2* ($n = 13$) and Δ*pilX3* ($n = 13$) mutants was determined. The deletion mutant Δ*hfq* lacking T4P was used as a negative control. Transformations were performed with different amounts of DNA ranging from 500 ng to 1 µg and different plasmids conferring different antibiotic resistances

(Figure S11). These proteins all form the hydrophobic N-terminal helix (Figure S11), which is the most conserved trait within pilins (Giltner et al., 2012) and thus is essential for the insertion of pilins into the fiber. We surmise, that at least PilA5, PilA6 and PilA10 can be incorporated into the pilus fiber like PilA4 (Cengic et al., 2018) due to the conservation of the hydrophobic handle. Moreover, secondary structure prediction (Figure S12) indicated hydrophobic handles for all known *Synechocystis* pilins and thus, all might be incorporated.

In addition to the assumption that PilA5 is incorporated into the pilus fiber, our results suggested that this protein facilitates DNA binding. However, we were not able to detect typical DNA binding motifs (Luscombe et al., 2000) or a region with enriched positively

charged amino acids in the PilA5 sequence, as was shown for the minor pilin ComP of *Neisseria meningitidis* (Berry et al., 2016). In this study, the researchers identified a region with a highly positively charged surface, which is probably involved in the electrostatic attraction of negatively charged DNA. For *Thermus thermophilus*, recent studies demonstrated that this naturally competent, gram-negative bacterium assembles two distinct T4P filaments composed of two different pilins. The wider filament is required for natural competence, whereas the more narrow one is used for twitching motility (Neuhaus et al., 2020). For *Synechocystis*, we did not obtain evidence from electron microscopy indicating that the different minor pilins form distinct pili (Figure S3). Additionally, our analysis of the general amount of the major pilin PilA1 in sheared pili fractions did not indicate a major difference in the level of piliation of the minor pilin mutants in comparison to the WT (Figure 6). These findings are supported by exoproteome analyses, which showed that the major pilin PilA1 is considerably more abundant in the exoproteome than minor pilins (Sergeyenko & Los, 2000). Therefore, we suggest that the minor pilins might be incorporated within a filament that is primarily composed of PilA1.

TABLE 3 Summary of mutant phenotypes

Strain	T4P	Motility	Natural competence	Flocculation
WT	+[c]	+[b]	+[a]	+[d]
Δ*pilA1*	−[c]	−[c]	−[c]	+[d]
Δ*pilA9-slr2019*	+	−[e]	+	−[d]
Δ*pilA5-pilA6*	+	+[c]	−	+
Δ*pilX1*	+	+	+	−
Δ*pilX2*	+	+/−	+	−
Δ*pilX3*	+	+	+	−

Note: Phenotypes of major and minor pilin mutants which have been analyzed in this and other studies.

[a]Grigorieva and Shestakov (1982).

[b]Bhaya et al. (1999).

[c]Yoshihara et al. (2001).

[d]Conradi et al. (2019).

[e]Wallner et al. (2020).

Taton et al. (2020) recently discovered indispensable proteins (minor pilin $PilA3_{S.e}$., $RntA_{S.e}$. and $RntB_{S.e}$) for natural transformation of the cyanobacterium *Synechococcus elongatus* PCC 7942. $RntB_{S.e}$. and $PilA3_{S.e}$. exhibit modest homology to the PilA5 and PilA6 proteins of *Synechocystis* (e-values between 1×10^{-04} and 4×10^{-06}, Table S2). $RntA_{S.e}$. shows homology to the PilX domain containing minor pilin PilX1 (Table S2). Notably, we also found a PilX-N domain in Slr2018 which is encoded by the *pilA9-slr2019* gene cluster (Figure S7; CDvist; HHsearch probability >95%). The protein Slr2018 might therefore be a PilX-like protein or an additional minor pilin (proposed by Chandra et al., 2017) of unusually large size (773 aa). Nevertheless, a multiple sequence alignment shows that the hydrophobic regions of PilX1, PilX2 and PilX3 are much more conserved to each other than to the hydrophobic region of Slr2018 (Figure 1b). Generally, PilX amino acid sequences are longer than those of the major pilin which is also true for the *Synechocystis* PilX-like proteins (Figure 1b). Although PilX from *Pseudomonas* lacks glutamate at position +5 (E_{+5}) of the PilD cleavage site, it was shown to be incorporated into the pilus fiber (Giltner et al., 2010). Pilins with substitution of E_{+5} to V_{+5} can still be cleaved and methylated (Strom & Lory, 1991). Moreover, it was hypothesized that pilins with a non-polar substitution have an improved ability to leave the membrane during assembly (Giltner et al., 2012). Thus, these proteins were proposed to form the pilus tip complex. This property was shown for the minor pilin GspK of the type II secretion complex of *E. coli*,

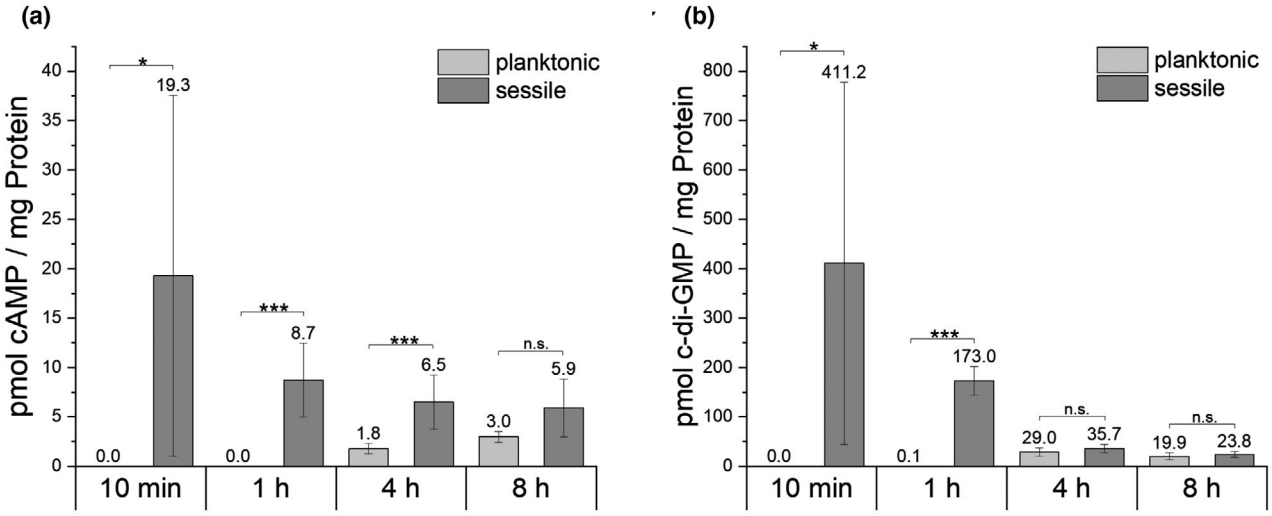

FIGURE 10 Intracellular cyclic nucleotide messenger concentrations in planktonic or sessile-grown *Synechocystis* WT cells. A planktonic preculture was cultivated either under planktonic or sessile conditions, and cAMP (a) and c-di-GMP (b) concentrations were determined after 10 min, 1, 4 and 8 hr. The bars display the mean concentration of cyclic nucleotide concentration normalized to whole cell protein amount. Error bars represent standard deviation. Experiments were performed as biological and extraction technical replicates. Significance was tested using a two-tailed Student's *t* test. $^{*}p \leq .05$, $^{**}p \leq .01$, $^{***}p \leq .001$, n.s., not significant

which also lacks E_{+5} (Korotkov & Hol, 2008), and a similar PilX minor pilin found in *Acinetobacter baumannii* T4P (Piepenbrink, 2019). The three *Synechocystis* PilX homologues also have different hydrophobic amino acid substitutions at position E_{+5} (Figure 1b). Additionally, secondary structure predictions indicated the existence of hydrophobic N-terminal helices, which are characteristic of minor pilins and are vital for insertion into the pilus (Figure S12). At the moment we are not able to predict where the *Synechocystis* minor pilins are positioned within the pilus fiber.

How are the minor pilins of *Synechocystis* involved in flocculation? There are many examples in bacteria and archaea which demonstrate cellular binding properties of T4P (reviewed in Giltner et al., 2012). Such species-specific cellular aggregation properties can be mediated by the interaction with sugars which are bound to surface structures (e.g., van Wolferen et al., 2020). In *Synechocystis*, a new sulfated exopolysaccharide, called synechan has been described which is essential for the formation of bloom-like cell aggregates (Maeda et al., 2021). The genes encoding proteins involved in synechan synthesis and regulation, all but one are located on the pSYSM plasmid in a large cluster (*sll5042-sll5060*). Several of these mRNAs represent the most differentially regulated mRNAs in our microarray analysis (Table 2). Most interestingly, the respective mRNAs accumulate strongly in the planktonic culture when compared to the cells on a surface, similar to the *pilA9-slr2019* and *pilX2* mRNAs. Thus, the exopolysaccharide synechan as well as this specific set of minor pilins are expressed under the same conditions and are essential for cell-cell interaction. Therefore, it is tempting to speculate that these minor pilins can bind specifically the sulfated exopolysaccharide to form together bloom-like cellular assemblages or flocs. Alternatively, T4P pili could also self-interact as it was shown, e.g., for the DNA-uptake pili of *Vibrio cholerae* (Adams et al., 2019). Here, the ability to aggregate in planktonic cultures was shown to depend on PilA variants which are encoded by different *Vibrio cholerae* isolates. T4P in *Vibrio cholerae* bind to chitin as a surface substrate and to pili of neighboring cells, suggesting a function of T4P as a recognition hub. This raises the hypothesis that the wide variety of cyanobacterial minor pilins could fulfil similar functions in surface contact and cell-cell interactions. Specific recognition could be achieved by using either different sugars and/or specific amino acid sequence motifs of pilin variants.

4 | MATERIALS AND METHODS

4.1 | Bacterial strains and culture conditions

The WT of *Synechocystis* sp. PCC 6803 employed in this study is motile and can grow photoautotrophically, mixotrophically and chemoheterotrophically on glucose. This strain was originally obtained from S. Shestakov (Moscow State University, Russia) in 1993 and was re-sequenced in 2012 (Trautmann et al., 2012).

Cyanobacteria were cultivated under either sessile or planktonic conditions. Planktonic cultures were grown in modified 1 × BG11 (Rippka et al., 1979) substituted with 0.3% (w/v) sodium thiosulfate and 10 mM (w/v) (N-[tris-(hydroxymethyl)-methyl]-2-aminoethane sulphonic acid) buffer (TES) pH 8.0. Cultures were grown photoautotrophically with orbital shakers at 140 rpm at 30°C under continuous white light illumination (Philips TLD Super 80/840) of 50 μmol photons m^{-2} s^{-1}. Sessile cultures were grown on 0.75% agar plates (Bacto-Agar) using the same medium and growth conditions without shaking as described for planktonic cultures.

Cyanobacterial strains were cultivated on BG11 agar plates as described above, and antibiotics, if necessary, were added at the following concentrations: chloramphenicol, 14 μg/ml; kanamycin, 40 μg/ml; and gentamycin, 10 μg/ml. For cloning of plasmids, *E. coli* DH5α was used, which was grown in LB medium supplemented with antibiotics at the following concentrations: ampicillin, 100 μg/ml; streptomycin, 25 μg/ml; and gentamycin, 10 μg/ml.

4.2 | Construction of mutant strains

The deletion mutant Δ*pilA5-pilA6* was created as described in Wallner et al. (2020). Three plasmids were constructed bearing either the single gene *pilA5* or *pilA6* alone or the operon *pilA5-pilA6* under the control of the native promoter ($P_{pilA5\text{-}pilA6}$). For a list of oligonucleotides used to generate all mutant constructs, see Table S3. The gene fragments $P_{pilA5\text{-}pilA6}$-*pilA5* and $P_{pilA5\text{-}pilA6}$-*pilA5-pilA6* were amplified from WT chromosomal DNA with an SdaI recognition site at the 5′-end (P1-P3) and inserted into the pJET 1.2 vector (CloneJET PCR Cloning Kit, Thermo ScientificTM, Germany). For the third construct, assembly cloning (AQUA cloning) (Beyer et al., 2015) was used to fuse the pJET 1.2 vector with the $P_{pilA5\text{-}pilA6}$ fragment containing the SdaI recognition site at the 5′-end and the *pilA6* gene fragment (P4-P9). The subcloning vectors were cleaved with SdaI and HindIII restriction enzymes, and fragments were ligated into the pVZ322 vector (NCBI accession number AF100175), which was cleaved with the same restriction enzymes. The final plasmids were transferred into the *Synechocystis* deletion mutant Δ*pilA5-pilA6* via triparental mating (Elhai & Wolk, 1988) with *E. coli* J53 (NCBI:txid1144303) harbouring the conjugative helper plasmid RP4 (NCBI:txid2503) and *E. coli* DH5α with the constructed plasmid. Verification of correct mutant strains was validated by PCR using primer pair P10-P11 (Figure S1). A list of all plasmids and strains used in this study can be found in Tables S4 and S5.

A *Synechocystis* knockout mutant of the *slr5087-slr5088* operon located on the pSYSM plasmid was generated (Figure S1d). First, we amplified chromosomal regions to be used as homologous recombination sites and added a NsiI restriction site to homologous region 1 (HR1) and overlapping regions using primer pairs P12-P13 and P14-P15. A combined homologous region sequence was obtained by overlap PCR using the two amplified DNA fragments and primer pair P12-P15. The construct was inserted into the pJET1.2 vector according to the manufacturer's instructions (CloneJET PCR Cloning Kit, Thermo ScientificTM, Germany). Furthermore, a chloramphenicol resistance cassette was amplified from the pACYC184

vector (GenBank: X06403.1), and NsiI restriction sites were added (P16-P17). This amplification product and the vector were cleaved by NsiI and ligated using T4 DNA ligase (New England BioLabs, Inc.). Insert orientation was checked by sequencing. Finally, *Synechocystis* WT was transformed with the plasmid. DNA of the mutants was extracted from cells by three repeated cycles of shock freezing (−80°C) and heating (60°C) for 10 min each. DNA was separated from cell debris by centrifugation at 3,000*g* for 3 min at 4°C. Correct construct insertion and full segregation were tested by colony PCR using the primer pair P18-P19 (Figure S1e).

Deletion mutants of *pilX* genes (Δ*pilX1*, Δ*pilX2*, Δ*pilX3*) were generated using a plasmid assembled via AQUA cloning (Figure S8a). The plasmid backbones were amplified from pJET 1.2 vector (CloneJET PCR Cloning Kit, Thermo ScientificTM, Germany) with primer pairs P20-P21, P22-P23 and P24-P25. Homologous recombination sites were amplified from *Synechocystis* WT genomic DNA with primer pairs P26-P27 and P28-P29, P30-P31 and P32-P33 and P34-P35 and P36-P37. Kanamycin resistance cassette was amplified from a pVZ321 (NCBI:txid88282) derived plasmid with primer pairs P38-P39, P40-P41 and P42-P43. WT *Synechocystis* cells were transformed with the corresponding plasmid. DNA was extracted as described above and construct insertion as well as complete segregation were tested by Colony PCR using primer pairs P44-P45 & P44-P46, P47-P48 & P48-P49 and P50-P51 & P51-P52 (Figure S8b).

4.3 | Flocculation assays

Flocculation assays were mainly performed as described in Conradi et al. (2019). Briefly, cultures were diluted to an OD_{750nm} 0.25, and 6 ml were transferred to 6-well plates (Corning Costar®, non-treated, 392-0213, VWR, Germany). Cultures were incubated for 48 hr at 30°C and 40 μmol photons m^{-2} s^{-1} of white light at 95 rpm on an orbital shaker. Images were taken by measuring chlorophyll autofluorescence using a Typhoon FLA4500 imaging system (GE Healthcare) with laser excitation at 473 nm and fluorescence detection at 665 nm. The aggregation score was calculated by dividing the standard deviation by the mean intensity as described in Conradi et al. (2019).

4.4 | Transformation assays

Natural transformation competence was tested with a suicide plasmid encoding streptomycin resistance. Cells were grown to log phase (OD_{750nm} 0.6 – 0.8) in planktonic culture, and 15 ml were harvested by centrifugation (3,200*g*, RT). The cell pellet was resuspended in 300 μl BG11 medium. Then, 500 or 1,000 ng of plasmid DNA were added to the suspension, and cultures were incubated at 30°C under white light (≈ 50 μmol photons m^{-2} s^{-1}) without shaking. After three hours, cells were plated on sterile filters (0.2 μm pore size, MN615, Macherey-Nagel), placed on BG11 agar plates and incubated under standard conditions. After two days, the filters were transferred to new BG11 agar plates supplemented with 5 μg/ml streptomycin and incubated further until colonies appeared. Alternatively, instead of transferring the cells to the filter, they were streaked directly on an BG-11 agar plate. Then, a small filter paper (ø 2.9 cm) was placed in the middle of the plate and 25 μl of a streptomycin solution (25 μg/ml) were added onto the filter to create a concentration gradient of the antibiotic. Plates were incubated as described above. Integration of the construct used led to deletion of the sRNA gene *psrR1*, which had no phenotypical effect under normal cultivation conditions (Georg et al., 2014).

4.5 | Transmission electron microscopy

Strains WT, Δ*hfq*, Δ*pilA5-pilA6* and Δ*pilA9-slr2019* were grown in BG-11 medium under continuous white light conditions (40–50 μmol photons m^{-2} s^{-1}) at 28°C for 2 days to an OD730nm 0.7–0.8. Cells were dropped onto formvar-coated grids, negatively stained with 1% aqueous uranyl acetate (w/v) according to Harris (1997) and examined by a Jeol 1010 transmission electron microscope operated at 80 kV equipped with a Mega View III camera (SIS). Acquired pictures were analyzed with ImageJ (Abramoff et al., 2004).

Strains Δ*pilX1*, Δ*pilX2* and Δ*pilX3* were taken from standard BG-11 plates and resuspended to low OD. Then 10 μl of cells were applied on a glow-discharged 300 mesh formvar and carbon-coated copper grid (Plano GmbH) and incubated for 10 min. The excess liquid was blotted away and then the grids were washed three times with 10 μl ultrapure H_2O. Afterwards the cells were stained with 2% (w/v) uranyl acetate for 5 min. Grids were washed once more and then dried completely. Imaging was performed using Zeiss Leo 912 Omega (Tungsten) operated at 80 kV. Images were taken with Dual Speed 2K-On-Axis charged-coupled device (CCD) camera (TRS, Sharp-Eye).

4.6 | Pili quantification

Cells were plated on standard BG11 plates supplemented with 0.2% glucose and grown under standard growth conditions (see above). After 6 days, cells were scratched from the surface, resuspended in phosphate-buffered saline (PBS; pH 7.4) and vortexed for 1 min. The concentration for each sample was adjusted to $OD_{750} = 10$. Cells and cell debris were collected for 5 min and washed for 10 min by centrifugation at 18,570*g*. The supernatants were supplemented with 1/10 V 5 M NaCl and 30% polyethylene glycol (PEG; MW 8000). Pili were precipitated at 4°C overnight and collected by centrifugation at 21,000*g* at 4°C for 1 hr. To achieve a uniform resuspension in SDS-loading buffer, the samples were heated to 50°C for 45 min and frozen at −20°C. 10 μl of protein samples were separated on a 15% SDS-PAGE gel and blotted onto a nitrocellulose membrane with Towbin-buffer (25 mM Tris, 192 mM glycine (pH 8.3), 20% methanol). After the transfer, the membrane was blocked with 5% milk powder at ambient temperature for 1 hr and washed three times

with TBS-T (150 mM NaCl, 20 mM Tris (pH 7.6), 0.1% Tween). The membrane was incubated with an anti-PilA1 antibody (kindly provided by Roman Sobotka) at 4°C over night, washed three times with TBS-T and incubated with the secondary antibody (goat anti-rabbit HRP antibody; Pierce, Thermo Fisher Scientific) at ambient temperature for 2 hr. The membrane was washed again three times with TBS-T and developed with Pierce™ ECL Plus Western blotting substrate (Thermo Fisher Scientific, Germany) and imaged with a Fusion imager (Vilber, Germany). Quantification was performed using the Fiji (ImageJ) software.

4.7 | Fluorescent bead assay

Fluorescent bead assays were performed as described in Nakane and Nishizaka (2017) with slight changes. The coverslip was prepared as described by Nakane and Nishizaka (2017) but coated with 4% (v/v) collodion in isoamyl acetate. Cells were added and incubated for 10 min, and then unattached cells were removed by rinsing with BG11. Coverslips were transferred to the microscope stage and illuminated for 2 min with red light (λ_{max} = 640 nm). Then, 0.2 μm fluorescent polystyrene beads (F8848, Thermo Fisher Scientific, Germany, final concentration 0.02% (w/v) in BG11) were added, and the fluorescent signal was detected by excitation at 426–450 nm, cut off at 458 nm and detected at 467–499 nm with an upright microscope (Nikon Instruments, Japan).

4.8 | Phototaxis experiments

Phototactic movement of cyanobacterial cells was analyzed on 0.5% agar plates containing BG11, 10 mM (w/v) TES buffer (pH 8.0), 0.3% (w/v) sodium thiosulphate and 11 mM glucose as previously described by Jakob et al. (2017). Cells were concentrated in a small volume of BG11, and 7 μl of cell suspension were spotted as droplets in triplicate on the phototaxis plate. Plates were then illuminated with unidirectional white light (≈5 μmol photons m^{-2} s^{-1}) and incubated for 6–7 days at 30°C. Pictures were taken with a flatbed scanner.

4.9 | RNA extraction

A planktonic preculture was grown in BG11 medium to OD_{750nm} 0.6–0.8. Then, 35 ml were centrifuged at 4,000*g* for 10 min at room temperature. For planktonic cultures, pellets were resuspended in 35 ml BG11 medium and incubated as described above in the culture conditions section. For sessile cultures, pellets were resuspended in 300 μl BG11 medium, plated onto BG11 agar plates and incubated as described above in the culture conditions section. After 10 min, 1, 4 or 8 hr RNA was harvested. For planktonic cultures, cells were collected by vacuum filtration through 0.8 μm polyethersulphone filter disks (Pall, Germany). Filters were immediately transferred to 1.6 ml PGTX solution (Pinto et al., 2009), vortexed, frozen in liquid nitrogen and stored at −80°C until further use. For sessile cultures, cells were scratched from the agar plates and directly suspended in 1.6 ml PGTX solution, vortexed, frozen in liquid nitrogen and stored at −80°C. RNA was then extracted according to Pinto et al. (2009) with modifications as described in Wallner et al. (2020).

4.10 | Microarray analysis

Removal of potential DNA from the RNA samples was performed using Ambion TurboDNase (Thermo Fisher Scientific, Germany) according to the manufacturer's instructions, but addition and incubation with Turbo DNase were performed twice. RNA was precipitated overnight with 3 M sodium acetate (pH 5.2) in 97% (v/v) ethanol. Furthermore, RNA was collected by centrifugation at 20,800*g* for 30 min, washed with 70% ethanol and eluted in nuclease-free water. The concentration was checked on a NanoDrop ND2000 spectrophotometer (Thermo Fisher Scientific, Germany), and integrity was verified using a fragment analyser (Advanced Analytical Technologies, Germany). Furthermore, RNA was labelled with Cy3 (ULSTM Fluorescent Labeling Kit for Agilent Arrays (EA-023), Kreatech, Germany), fragmented, and 600 ng were hybridized with a high-resolution custom-made microarray (Agilent Technologies, Germany, Design ID 075764, format 8 × 60 K; slide layout = IS-62976-8-V2) in duplicates. The full dataset is available in the database NCBI's Gene Expression Omnibus and accessible through GEO Series accession number GSE161586 (https://www.ncbi.nlm.nih.gov/geo/query/acc.cgi?acc=GSE161586). Further, the analyzed dataset, containing all coding and non-coding RNAs can be found in the Supplementary Data Table. Graphical visualizations of the microarray results for the chromosome and all large plasmids are available in data sets S1–S5.

4.11 | Northern blot hybridization

Northern blot hybridizations were performed. RNA was extracted as described above. Seven or ten micrograms of RNA was separated on a denaturing 1.3% (w/v) agarose-formaldehyde electrophoresis gel and blotted onto a Roti-Nylon plus membrane (Carl Roth, Germany). The Northern blot was hybridized with probes generated by in vitro transcription of PCR fragments (P53-P60, Table S3) using radioactively labelled [α-^{32}P]-UTP and the Ambion T7 polymerase Maxiscript kit (Thermo Fisher Scientific, Germany). Signals were detected by phosphoimaging on a Typhoon FLA4500 imaging system (GE Healthcare).

4.12 | Extraction of nucleotide second messengers

Cells for planktonic and sessile cultures were grown the same way as described for RNA extraction. To obtain measurable amounts of second messengers for sessile cultures, cells from two plates

were scratched and suspended in 250 µl BG11 medium. Cells from 50 µl of this suspension were pelleted at 11,000*g* at 4°C for 2 min for nucleotide extraction, and 50 µl were pelleted and used for determination of protein concentration. For planktonic samples, 10 ml of a liquid cell culture were pelleted for nucleotide and 1 ml for protein quantification. Cell pellets were resuspended in 300 µl extraction solution (acetonitrile/methanol/water 2:2:1 [v/v/v]), incubated at 4°C for 15 min and heated to 95°C for 10 min. Samples were snap-cooled on ice and stored for further use at −20°C or centrifuged at 21,000*g* at 4°C for 10 min, and the supernatant was collected. The extraction was repeated twice from the pellets with 200 µl extraction solution each, without heat treatment. Supernatants were combined, and proteins precipitated by incubation at −20°C overnight. The samples were centrifuged at 21,000*g* at 4°C for 10 min, and the supernatant containing the extracted second messengers was air dried in a SpeedVac at 42°C. Quantification of c-di-GMP and cAMP was performed by HPLC/MS/MS analysis, as previously described (Burhenne & Kaever, 2013). Second messengers were normalized to the total protein amount. For protein quantification, cell pellets were resuspended in 50 µl PBS, supplemented with 0.7 volume of glass bead mix (0.1–0.11 and 0.25–0.5 mm) and vortexed for 60 s. Then, the samples were snap-cooled at −80°C twice and heated to 40°C for 10 min each. After sedimentation of the beads, 2 µl of the supernatant were used for protein quantification using the Direct Detect system (Merck Millipore).

4.13 | Bioinformatic analysis

All bioinformatic tools used are listed in Table S6.

ACKNOWLEDGEMENTS

We thank D. Nakane (Gakushuin University), who established the bead assay in our lab, and A. Jakob (University of Freiburg) for performing the assays together with S. Oeser. We acknowledge V. Reimann and W. Bigott (both University of Freiburg) for help with microarray analysis and Northern Blots hybridizations. We are grateful to the students S. Klostermayer and A. Moellering for experimental contributions and F. Conradi and C. W. Mullineaux for valuable discussions. We thank R. Sobotka (Institute of Microbiology of the Czech Academy of Sciences) for scientific exchange and the antibody against PilA1. We acknowledge the Laboratory of Electron Microscopy, the core facility of Biology Centre of CAS supported by the MEYS CR (LM2015062 Czech-BioImaging). The other TEM is operated by the University of Freiburg, Faculty of Biology, as a partner unit within the Microscopy and Image Analysis Platform, Freiburg. This work was supported by grants to A. Wilde of the German Science Foundation (DFG) as part of DFG Priority Programme SPP1879 (Wi 2014/7-1) and the SFB 1381 (Deutsche Forschungsgemeinschaft [German Research Foundation] under project no. 403222702-SFB 1381) to A. Wilde (A2) and S.-V. Albers (A1). Open access funding enabled and organized by ProjektDEAL.

CONFLICT OF INTEREST

The authors declare that the research was conducted in the absence of any commercial or financial relationships that could be construed as a potential conflict of interest.

AUTHOR CONTRIBUTIONS

SO performed experiments, analyzed and interpreted the data, wrote the manuscript and contributed to the design of the study. TW performed experiments, interpreted the data and contributed to the design of the study. NS performed experiments, interpreted the data and contributed to the design of the study. LB performed experiments and analyzed data. SS performed experiments with SO and analyzed the data. SVA interpreted the data and contributed to the design of the study. AW contributed to the design of the study, interpreted data and wrote the manuscript.

DATA AVAILABILITY STATEMENT

The data that support the findings of this study are openly available in NCBI's Gene Expression Omnibus at https://www.ncbi.nlm.nih.gov/geo/query/acc.cgi?acc=GSE161586, reference number GSE161586.

ORCID

Thomas Wallner https://orcid.org/0000-0002-8198-8465
Sonja-Verena Albers https://orcid.org/0000-0003-2459-2226
Annegret Wilde https://orcid.org/0000-0003-0935-8415

REFERENCES

Abramoff, M.D., Magalhaes, P.J. & Ram, S.J. (2004) Image processing with ImageJ. *Biophotonics International*, *11*, 36–42.

Adams, D.W., Stutzmann, S., Stoudmann, C. & Blokesch, M. (2019) DNA-uptake pili of *Vibrio cholerae* are required for chitin colonization and capable of kin recognition via sequence-specific self-interaction. *Nature Microbiology*, *4*, 1545–1557. https://doi.org/10.1038/s41564-019-0479-5

Agostoni, M., Koestler, B.J., Waters, C.M., Williams, B.L. & Montgomery, B.L. (2013) Occurrence of cyclic di-GMP-modulating output domains in cyanobacteria: an illuminating perspective. *mBio*, *4*, 451–464. https://doi.org/10.1128/mBio.00451-13

Agostoni, M., Waters, C.M. & Montgomery, B.L. (2016) Regulation of biofilm formation and cellular buoyancy through modulating intracellular cyclic di-GMP levels in engineered cyanobacteria. *Biotechnology and Bioengineering*, *113*, 311–319. https://doi.org/10.1002/bit.25712

Aldridge, C., Spence, E., Kirkilionis, M.A., Frigerio, L. & Robinson, C. (2008) Tat-dependent targeting of Rieske iron-sulphur proteins to both the plasma and thylakoid membranes in the cyanobacterium *Synechocystis* PCC 6803. *Molecular Microbiology*, *70*, 140–150. https://doi.org/10.1111/j.1365-2958.2008.06401.x

Barten, R. & Lill, H. (1995) DNA-uptake in the naturally competent cyanobacterium, *Synechocystis* sp. PCC 6803. *FEMS Microbiology Letters*, *129*, 83–87.

Belete, B., Lu, H. & Wozniak, D.J. (2008) *Pseudomonas aeruginosa* AlgR regulates type IV pilus biosynthesis by activating transcription of the *fimU-pilVWXY1Y2E* operon. *Journal of Bacteriology*, *190*, 2023–2030.

Berry, J.L., Xu, Y., Ward, P.N., Lea, S.M., Matthews, S.J. & Pelicic, V. (2016) A comparative structure/function analysis of two type IV pilin DNA receptors defines a novel mode of DNA binding. *Structure*, *24*, 926–934. https://doi.org/10.1016/j.str.2016.04.001

Beyer, H.M., Gonschorek, P., Samodelov, S.L., Meier, M., Weber, W. & Zurbriggen, M.D. (2015) AQUA cloning: a versatile and simple enzyme-free cloning approach. *PLoS One*, *10*, e0137652. https://doi.org/10.1371/journal.pone.0137652

Bhaya, D., Bianco, N.R., Bryant, D. & Grossman, A. (2000) Type IV pilus biogenesis and motility in the cyanobacterium *Synechocystis* sp. PCC6803. *Molecular Microbiology*, *37*, 941–951.

Bhaya, D., Takahashi, A., Shahi, P. & Grossman, A.R. (2001) Novel motility mutants of *Synechocystis* strain PCC 6803 generated by in vitro transposon mutagenesis. *Journal of Bacteriology*, *183*, 6140–6143.

Bhaya, D., Watanabe, N., Ogawa, T. & Grossman, A.R. (1999) The role of an alternative sigma factor in motility and pilus formation in the cyanobacterium *Synechocystis* sp. strain PCC 6803. *Proceedings of the National Academy of Sciences of the United States of America*, *96*, 3188–3193. https://doi.org/10.1073/pnas.96.6.3188

Burhenne, H. & Kaever, V. (2013) Quantification of cyclic dinucleotides by reversed-phase LC-MS/MS. *Methods in Molecular Biology*, *1016*, 27–37.

Cehovin, A., Simpson, P.J., McDowell, M.A., Brown, D.R., Noschese, R., Pallett, M. et al. (2013) Specific DNA recognition mediated by a type IV pilin. *Proceedings of the National Academy of Sciences of the United States of America*, *110*, 3065–3070. https://doi.org/10.1073/pnas.1218832110

Cengic, I., Uhlén, M. & Hudson, E.P. (2018) Surface display of small affinity proteins on *Synechocystis* sp. strain PCC 6803 mediated by fusion to the major type IV pilin PilA1. *Journal of Bacteriology*, *200*, e00270-18.

Chandra, A., Joubert, L.-M. & Bhaya, D. (2017) Modulation of type IV pili phenotypic plasticity through a novel chaperone-usher system in *Synechocystis* sp. *bioRxiv*, 130278.

Conradi, F.D., Zhou, R.Q., Oeser, S., Schuergers, N., Wilde, A. & Mullineaux, C.W. (2019) Factors controlling floc formation and structure in the cyanobacterium *Synechocystis* sp. strain PCC 6803. *Journal of Bacteriology*, *201*, e00344-19.

DeFlaun, M.F., Paul, J.H. & Davis, D. (1986) Simplified method for dissolved DNA determination in aquatic environments. *Applied and Environment Microbiology*, *52*, 654–659. https://doi.org/10.1128/aem.52.4.654-659.1986

Denise, R., Abby, S.S. & Rocha, E.P.C. (2019) Diversification of the type IV filament superfamily into machines for adhesion, protein secretion, DNA uptake, and motility. *PLoS Biology*, *17*, e3000390. https://doi.org/10.1371/journal.pbio.3000390

Dienst, D., Dühring, U., Mollenkopf, H.-J., Vogel, J., Golecki, J., Hess, W.R. et al. (2008) The cyanobacterial homologue of the RNA chaperone Hfq is essential for motility of *Synechocystis* sp. PCC 6803. *Microbiology*, *154*, 3134–3143. https://doi.org/10.1099/mic.0.2008/020222-0

Eisenhut, M., Wobeser, E.A.V., Jonas, L., Schubert, H., Ibelings, B.W., Bauwe, H. et al. (2007) Long-term response toward inorganic carbon limitation in wild type and glycolate turnover mutants of the cyanobacterium *Synechocystis* sp. strain PCC 6803. *Plant Physiology*, *144*, 1946–1959.

Elhai, J. & Wolk, C.P.P. (1988) Conjugal transfer of DNA to cyanobacteria. *Methods in Enzymology*, *167*, 747–754.

Ellison, C.K., Dalia, T.N., Vidal Ceballos, A., Wang, J.-C.-Y.-Y., Biais, N., Brun, Y.V. et al. (2018) Retraction of DNA-bound type IV competence pili initiates DNA uptake during natural transformation in *Vibrio cholerae*. *Nature Microbiology*, *3*, 773–780. https://doi.org/10.1038/s41564-018-0174-y

Georg, J., Dienst, D., Schürgers, N., Wallner, T., Kopp, D., Stazic, D. et al. (2014) The small regulatory RNA SyR1/PsrR1 controls photosynthetic functions in cyanobacteria. *The Plant Cell*, *26*, 3661–3679. https://doi.org/10.1105/tpc.114.129767

Giltner, C.L., Habash, M. & Burrows, L.L. (2010) *Pseudomonas aeruginosa* minor pilins are incorporated into type IV pili. *Journal of Molecular Biology*, *398*, 444–461. https://doi.org/10.1016/j.jmb.2010.03.028

Giltner, C.L., Nguyen, Y. & Burrows, L.L. (2012) Type IV pilin proteins: versatile molecular modules. *Microbiology and Molecular Biology Reviews*, *76*, 740–772. https://doi.org/10.1128/MMBR.00035-12

Giner-Lamia, J., Robles-Rengel, R., Hernández-Prieto, M.A., Isabel Muro-Pastor, M., Florencio, F.J. & Futschik, M.E. (2017) Identification of the direct regulon of NtcA during early acclimation to nitrogen starvation in the cyanobacterium *Synechocystis* sp. PCC 6803. *Nucleic Acids Research*, *45*, 11800–11820. https://doi.org/10.1093/nar/gkx860

Gordon, V.D. & Wang, L. (2019) Bacterial mechanosensing: the force will be with you, always. *Journal of Cell Science*, *132*, jcs227694. https://doi.org/10.1242/jcs.227694

Grigorieva, G. & Shestakov, S. (1982) Transformation in the cyanobacterium *Synechocystis* sp. 6803. *FEMS Microbiology Letters*, *13*, 367–370.

Harris, J.R. (1997) Negative staining and cryo-electron microscopy: the thin film techniques. In *RMS*, *Microscopy Handbook*. BIOS Scientific Publishers Ltd.

Hengge, R. (2021) High-specificity local and global c-di-GMP signaling. *Trends in Microbiology*, *24*, S0966-842X(21)00037-8. Epub ahead of print.

Hernández-Prieto, M.A., Semeniuk, T.A., Giner-Lamia, J. & Futschik, M.E. (2016) The transcriptional landscape of the photosynthetic model cyanobacterium *Synechocystis* sp. PCC 6803. *Scientific Reports*, *6*, 1–15. https://doi.org/10.1038/srep22168

Hu, J., Zhan, J., Chen, H., He, C., Cang, H. & Wang, Q. (2018) The small regulatory antisense RNA PilR affects pilus formation and cell motility by negatively regulating *pilA11* in *Synechocystis* sp. PCC 6803. *Frontiers in Microbiology*, *9*, 786. https://doi.org/10.3389/fmicb.2018.00786

Ibáñez de Aldecoa, A.L., Zafra, O. & González-Pastor, J.E. (2017) Mechanisms and regulation of extracellular DNA release and its biological roles in microbial communities. *Frontiers in Microbiology*, *8*, 1390. https://doi.org/10.3389/fmicb.2017.01390

Jacobsen, T., Bardiaux, B., Francetic, O., Izadi-Pruneyre, N. & Nilges, M. (2020) Structure and function of minor pilins of type IV pili. *Medical Microbiology and Immunology*, *209*, 301–308. https://doi.org/10.1007/s00430-019-00642-5

Jakob, A., Schuergers, N. & Wilde, A. (2017) Phototaxis assays of *Synechocystis* sp. PCC 6803 at macroscopic and microscopic scales. *Bio-Protocol*, *7*, e2328.

Kaneko, T., Nakamura, Y., Sasamoto, S., Watanabe, A., Kohara, M., Matsumoto, M. et al. (2003) Structural analysis of four large plasmids harboring in a unicellular cyanobacterium, *Synechocystis* sp. PCC 6803. *DNA Research*, *10*, 221–228. https://doi.org/10.1093/dnares/10.5.221

Kizawa, A., Kawahara, A., Takimura, Y., Nishiyama, Y. & Hihara, Y. (2016) RNA-seq profiling reveals novel target genes of LexA in the cyanobacterium *Synechocystis* sp. PCC 6803. *Frontiers in Microbiology*, *7*, 193. https://doi.org/10.3389/fmicb.2016.00193

Klotz, A., Georg, J., Bučinská, L., Watanabe, S., Reimann, V., Januszewski, W. et al. (2016) Awakening of a dormant cyanobacterium from nitrogen chlorosis reveals a genetically determined program. *Current Biology*, *26*, 2862–2872. https://doi.org/10.1016/j.cub.2016.08.054

Kopf, M., Klähn, S., Scholz, I., Matthiessen, J.K.F., Hess, W.R. & Voß, B. (2014) Comparative analysis of the primary transcriptome of *Synechocystis* sp. PCC 6803. *DNA Research*, *21*, 527–539. https://doi.org/10.1093/dnares/dsu018

Korotkov, K.V. & Hol, W.G.J. (2008) Structure of the GspK-GspI-GspJ complex from the enterotoxigenic *Escherichia coli* type 2 secretion system. *Nature Structural & Molecular Biology*, *15*, 462–468. https://doi.org/10.1038/nsmb.1426

Laventie, B.-J.-J. & Jenal, U. (2020) Surface sensing and adaptation in bacteria. *Annual Review of Microbiology*, *74*, 735–760. https://doi.org/10.1146/annurev-micro-012120-063427

Laventie, B.-J., Sangermani, M., Estermann, F., Manfredi, P., Planes, R., Hug, I. et al. (2019) A surface-induced asymmetric program promotes

tissue colonization by *Pseudomonas aeruginosa*. *Cell Host & Microbe*, *25*, 140–152.e6. https://doi.org/10.1016/j.chom.2018.11.008

Linhartová, M., Bučinská, L., Halada, P., Ječmen, T., Šetlík, J., Komenda, J. et al. (2014) Accumulation of the type IV prepilin triggers degradation of SecY and YidC and inhibits synthesis of photosystem II proteins in the cyanobacterium Synechocystis PCC 6803. *Molecular Microbiology*, *93*, 1207–1223.

Luscombe, N.M., Austin, S.E., Berman, H.M. & Thornton, J.M. (2000) An overview of the structures of protein-DNA complexes. *Genome Biology*, *1*(reviews001), 1.

Maeda K., Okuda Y., Enomoto G., Watanabe S., Ikeuchi M. (2021) Biosynthesis of a sulfated exopolysaccharide, synechan, and bloom formation in the model cyanobacterium *Synechocystis* sp. strain PCC 6803. *eLife*, *10*. http://dx.doi.org/10.7554/elife.66538

Mattick, J.S. (2002) Type IV pili and twitching motility. *Annual Review of Microbiology*, *56*, 289–314. https://doi.org/10.1146/annurev.micro.56.012302.160938

Mitschke, J., Georg, J., Scholz, I., Sharma, C.M., Dienst, D., Bantscheff, J. et al. (2011) An experimentally anchored map of transcriptional start sites in the model cyanobacterium *Synechocystis* sp. PCC 6803. *Proceedings of the National Academy of Sciences of the United States of America*, *108*, 2124–2129.

Nakane, D. & Nishizaka, T. (2017) Asymmetric distribution of type IV pili triggered by directional light in unicellular cyanobacteria. *Proceedings of the National Academy of Sciences of the United States of America*, *114*, 6593–6598. https://doi.org/10.1073/pnas.1702395114

Nakasugi, K., Svenson, C.J. & Neilan, B.A. (2006) The competence gene, *comF*, from *Synechocystis* sp. strain PCC 6803 is involved in natural transformation, phototactic motility and piliation. *Microbiology*, *152*, 3623–3631. https://doi.org/10.1099/mic.0.29189-0

Neuhaus, A., Selvaraj, M., Salzer, R., Langer, J.D., Kruse, K., Kirchner, L. et al. (2020) Cryo-electron microscopy reveals two distinct type IV pili assembled by the same bacterium. *Nature Communications*, *11*, 1–13.

Ng, D., Harn, T., Altindal, T., Kolappan, S., Marles, J.M., Lala, R. et al. (2016) The *Vibrio cholerae* minor pilin TcpB initiates assembly and retraction of the toxin-coregulated pilus. *PLoS Pathogens*, *12*, e1006109. https://doi.org/10.1371/journal.ppat.1006109

Nguyen, Y., Sugiman-Marangos, S., Harvey, H., Bell, S.D., Charlton, C.L., Junop, M.S. et al. (2015) *Pseudomonas aeruginosa* minor pilins prime type IVa pilus assembly and promote surface display of the PilY1 adhesin. *Journal of Biological Chemistry*, *290*, 601–611. https://doi.org/10.1074/jbc.M114.616904

Niemeyer, J. & Gessler, F. (2002) Determination of free DNA in soils. *Journal of Plant Nutrition and Soil Science*, *165*, 121. https://doi.org/10.1002/1522-2624(200204)165:2<121:AID-JPLN111112>3.0.CO;2-X

Ohmori, M. & Okamoto, S. (2004) Photoresponsive cAMP signal transduction in cyanobacteria. *Photochemical & Photobiological Sciences*, *3*, 503–511. https://doi.org/10.1039/b401623h

Omagari, K., Yoshimura, H., Suzuki, T., Takano, M., Ohmori, M. & Sarai, A. (2008) ΔG-based prediction and experimental confirmation of SyCRP1-binding sites on the *Synechocystis* genome. *FEBS Journal*, *275*, 4786–4795. https://doi.org/10.1111/j.1742-4658.2008.06618.x

Orf, I., Schwarz, D., Kaplan, A., Kopka, J., Hess, W.R., Hagemann, M. et al. (2016) CyAbrB2 contributes to the transcriptional regulation of low CO_2 acclimation in *Synechocystis* sp. PCC 6803. *Plant and Cell Physiology*, *57*, 2232–2243.

Paul, J.H., Jeffrey, W.H., David, A.W., DeFlaun, M.F. & Cazares, L.H. (1989) Turnover of extracellular DNA in eutrophic and oligotrophic freshwater environments of Southwest Florida. *Applied and Environment Microbiology*, *55*, 1823–1828. https://doi.org/10.1128/aem.55.7.1823-1828.1989

Pelicic, V. (2008) Type IV pili: E pluribus unum? *Molecular Microbiology*, *68*, 827–837. https://doi.org/10.1111/j.1365-2958.2008.06197.x

Persat, A., Inclan, Y.F., Engel, J.N., Stone, H.A. & Gitai, Z. (2015) Type IV pili mechanochemically regulate virulence factors in *Pseudomonas aeruginosa*. *Proceedings of the National Academy of Sciences of the United States of America*, *112*, 7563–7568.

Piepenbrink, K.H. (2019) DNA uptake by type IV filaments. *Frontiers in Molecular Biosciences*, *6*, 1. https://doi.org/10.3389/fmolb.2019.00001

Pinto, F.L., Thapper, A., Sontheim, W. & Lindblad, P. (2009) Analysis of current and alternative phenol based RNA extraction methodologies for cyanobacteria. *BMC Molecular Biology*, *10*, 79. https://doi.org/10.1186/1471-2199-10-79

Porcellinis, A.J.D., Klähn, S., Rosgaard, L., Kirsch, R., Gutekunst, K., Georg, J. et al. (2016) The non-coding RNA Ncr0700/PmgR1 is required for photomixotrophic growth and the regulation of glycogen accumulation in the cyanobacterium *Synechocystis* sp. PCC 6803. *Plant and Cell Physiology*, *57*, 2091–2103.

Rodesney, C.A., Roman, B., Dhamani, N., Cooley, B.J., Katira, P., Touhami, A. et al. (2017) Mechanosensing of shear by *Pseudomonas aeruginosa* leads to increased levels of the cyclic-di-GMP signal initiating biofilm development. *Proceedings of the National Academy of Sciences of the United States of America*, *114*, 5906–5911.

Rübsam, H., Kirsch, F., Reimann, V., Erban, A., Kopka, J., Hagemann, M. et al. (2018) The iron-stress activated RNA 1 (IsaR1) coordinates osmotic acclimation and iron starvation responses in the cyanobacterium *Synechocystis* sp. PCC 6803. *Environmental Microbiology*, *20*, 2757–2768.

Saha, C.K., Sanches Pires, R., Brolin, H., Delannoy, M., Atkinson, G.C., Pires, R.S. et al. (2020) FlaGs and webFlaGs: Discovering novel biology through the analysis of gene neighbourhood conservation. *Bioinformatics*, *37*, 1312–1314. btaa788.

Salleh, M.Z., Karuppiah, V., Snee, M., Thistlethwaite, A., Levy, C.W., Knight, D. et al. (2019) Structure and properties of a natural competence-associated pilin suggest a unique pilus tip-associated DNA receptor. *mBio*, *10*, e00614-19. https://doi.org/10.1128/mBio.00614-19

Savakis, P., Causmaecker, S.D., Angerer, V., Ruppert, U., Anders, K., Essen, L.-O. et al. (2012) Light-induced alteration of c-di-GMP level controls motility of *Synechocystis* sp. PCC 6803. *Molecular Microbiology*, *85*, 239–251. https://doi.org/10.1111/j.1365-2958.2012.08106.x

Schirmacher, A.M., Hanamghar, S.S. & Zedler, J.A.Z. (2020) Function and benefits of natural competence in cyanobacteria: From ecology to targeted manipulation. *Life*, *10*, 249. https://doi.org/10.3390/life10110249

Schlebusch, M. & Forchhammer, K. (2010) Requirement of the nitrogen starvation-induced protein Sll0783 for polyhydroxybutyrate accumulation in *Synechocystis* sp. strain PCC 6803. *Applied and Environment Microbiology*, *76*, 6101–6107.

Schuergers, N., Ruppert, U., Watanabe, S., Nürnberg, D.J., Lochnit, G., Dienst, D. et al. (2014) Binding of the RNA chaperone Hfq to the type IV pilus base is crucial for its function in *Synechocystis* sp. PCC 6803. *Molecular Microbiology*, *92*, 840–852.

Schuergers, N. & Wilde, A. (2015) Appendages of the cyanobacterial cell. *Life*, *5*, 700–715. https://doi.org/10.3390/life5010700

Sergeyenko, T.V. & Los, D.A. (2000) Identification of secreted proteins of the cyanobacterium *Synechocystis* sp. strain PCC 6803. *FEMS Microbiology Letters*, *193*, 213–216.

Shibata, M., Ohkawa, H., Katoh, H., Shimoyama, M. & Ogawa, T. (2002) Two CO_2 uptake systems in cyanobacteria: Four systems for inorganic carbon acquisition in *Synechocystis* sp. strain PCC 6803. *Functional Plant Biology*, *29*, 123–129. https://doi.org/10.1071/PP01188

Song, W.Y., Zang, S.S., Li, Z.K., Dai, G.Z., Liu, K., Chen, M. et al. (2018) SyCRP2 is essential for twitching motility in the cyanobacterium *Synechocystis* sp. strain PCC 6803. *Journal of Bacteriology*, *200*, e00436-18.

Stanier, R.Y., Deruelles, J., Rippka, R., Herdman, M. & Waterbury, J.B. (1979) Generic assignments, strain histories and properties of pure

cultures of cyanobacteria. *Journal of General Microbiology*, *111*, 1–61. https://doi.org/10.1099/00221287-111-1-1

Strom, M.S. & Lory, S. (1991) Amino acid substitutions in pilin of *Pseudomonas aeruginosa*. Effect on leader peptide cleavage, amino-terminal methylation, and pilus assembly. *Journal of Biological Chemistry*, *266*, 1656–1664. https://doi.org/10.1016/S0021-9258(18)52345-0

Taton, A., Erikson, C., Yang, Y., Rubin, B.E., Rifkin, S.A., Golden, J.W. et al (2020) The circadian clock and darkness control natural competence in cyanobacteria. *Nature Communications*, *11*, 1688. https://doi.org/10.1038/s41467-020-15384-9

Terauchi, K. & Ohmori, M. (1999) An adenylate cyclase, CyaI, regulates cell motility in the cyanobacterium *Synechocystis* sp. PCC 6803. *Plant and Cell Physiology*, *40*, 248–251. https://doi.org/10.1093/oxfordjournals.pcp.a029534

Torsvik, V.L. & Goksoyr, J. (1978) Determination of bacterial DNA in soil. *Soil Biology & Biochemistry*, *10*, 7–12. https://doi.org/10.1016/0038-0717(78)90003-2

Trautmann, D., Voß, B., Wilde, A., Al-Babili, S. & Hess, W.R. (2012) Microevolution in cyanobacteria: re-sequencing a motile substrain of *Synechocystis* sp. PCC 6803. *DNA Research*, *19*, 435–448. https://doi.org/10.1093/dnares/dss024

Treuner-Lange, A., Chang, Y.-W., Glatter, T., Herfurth, M., Lindow, S., Chreifi, G. et al. (2020) PilY1 and minor pilins form a complex priming the type IVa pilus in *Myxococcus xanthus*. *Nature Communications*, *11*, 1–14. https://doi.org/10.1038/s41467-020-18803-z

Trunk, T., Khalil, S.H. & Leo, J.C. (2018) Bacterial autoaggregation. *AIMS Microbiology*, *4*, 140–164.

van Wolferen, M., Shajahan, A., Heinrich, K., Brenzinger, S., Black, I.M., Wagner, A. et al. (2020) Species-specific recognition of *Sulfolobales* mediated by UV-inducible pili and S-layer glycosylation patterns. *mBio*, *11*, e03014-19.

Vorkapic, D., Pressler, K. & Schild, S. (2016) Multifaceted roles of extracellular DNA in bacterial physiology. *Current Genetics*, *62*, 71–79. https://doi.org/10.1007/s00294-015-0514-x

Wallner, T., Pedroza, L., Voigt, K., Kaever, V. & Wilde, A. (2020) The cyanobacterial phytochrome 2 regulates the expression of phototaxis-related genes through the second messenger cyclic di-GMP. *Photochemical & Photobiological Sciences*, *19*, 631–643.

Winther-Larsen, H.C., Hegge, F.T., Wolfgang, M., Hayes, S.F., Putten, J.P.M.V. & Koomey, M. (2001) *Neisseria gonorrhoeae* PilV, a type IV pilus-associated protein essential to human epithelial cell adherence. *Proceedings of the National Academy of Sciences of the United States of America*, *98*, 15276–15281. https://doi.org/10.1073/pnas.261574998

Wolfgang, M., Putten, J.P.M.V., Hayes, S.F. & Koomey, M. (1999) The *comP* locus of *Neisseria gonorrhoeae* encodes a type IV prepilin that is dispensable for pilus biogenesis but essential for natural transformation. *Molecular Microbiology*, *31*, 1345–1357. https://doi.org/10.1046/j.1365-2958.1999.01269.x

Yoshihara, S., Geng, XiaoXing, Okamoto, S., Yura, K., Murata, T., Go, M. et al. (2001) Mutational analysis of genes involved in pilus structure, motility and transformation competency in the unicellular motile cyanobacterium *Synechocystis* sp. PCC 6803. *Plant and Cell Physiology*, *42*, 63–73. https://doi.org/10.1093/pcp/pce007

Yoshimura, H., Yanagisawa, S., Kanehisa, M. & Ohmori, M. (2002) Screening for the target gene of cyanobacterial cAMP receptor protein SyCRP1. *Molecular Microbiology*, *43*, 843–853. https://doi.org/10.1046/j.1365-2958.2002.02790.x

Yoshimura, H., Yoshihara, S., Okamoto, S., Ikeuchi, M. & Ohmori, M. (2002) A cAMP receptor protein, SyYCRP1, is responsible for the cell motility of *Synechocystis* sp. PCC 6803. *Plant and Cell Physiology*, *43*, 460–463.

Yura, K., Toh, H. & Go, M. (1999) Putative mechanism of natural transformation as deduced from genome data. *DNA Research*, *6*, 75–82. https://doi.org/10.1093/dnares/6.2.75

SUPPORTING INFORMATION

Additional Supporting Information may be found online in the Supporting Information section.

How to cite this article: Oeser, S., Wallner, T., Schuergers, N., Bučinská, L., Sivabalasarma, S., Bähre, H., et al. (2021) Minor pilins are involved in motility and natural competence in the cyanobacterium *Synechocystis* sp. PCC 6803. *Molecular Microbiology*, 116, 743–765. https://doi.org/10.1111/mmi.14768